

FPGA-Based Data Acquisition System for Ultrasound Tomography

Michael Aitken

A project report submitted to the Department of Electrical Engineering,
University of Cape Town, in partial fulfilment of the requirements for the
degree of Bachelor of Science in Engineering.

Cape Town, October 2006

Declaration

I declare that this project report is my own, unaided work. It is being submitted for the degree of Bachelor of Science in Engineering at the University of Cape Town. It has not been submitted before for any degree or examination in any other university.

Signature of Author

Cape Town

22 October 2006

Abstract

Ultrasound Tomography involves the acquisition and analysis of large amounts of data, both of which must be done at high speed in order to be implemented in a mobile product. FPGA technology promises to provide the necessary parallel processing capabilities in order to accomplish various strenuous processing procedures. At the same time the technology allows a system to be designed and prototyped quickly and cost-effectively.

However, an FPGA device is limited by the speed at which it can acquire raw data. To facilitate ultrasound tomography, the external circuitry is responsible for acquiring high resolution data at high speeds that are sufficient in order to allow effective signal processing. The circuitry must also perform the opposite function, that being the ability to transform high resolution digital data into analogue signals at high speed.

This thesis sets out to investigate the recent developments in FPGA technology, looking specifically at the benefits that FPGAs deliver to embedded system design. It then moves on to suggest a software/hardware configuration that will provide a cheap, fast-tracked working demonstration of an ultrasound tomography system. It takes the reader through the process of building the entire system:

- designing and implementing the external hardware
- creating a customized soft-core Nios II processor
- interfacing all the system components
- writing the control code
- testing the system
- demonstrating valid results.

Lastly, and most importantly, since this project merely lays the foundation for further exploring FPGA technology, a range of possible project extensions are suggested.

This thesis is dedicated to my parents, who, even from so far away, gave me the love and support to get me this far.

I owe them more than can be imagined.

Acknowledgements

I would like to sincerely thank Dr A.J. Wilkinson for his proposal, his time, and his knowledgeable advice on this project. Thanks also go to Mr S. Ginsberg for his help in producing the PCB. Lastly, a thank you to my fellow lab mates for the jokes, the distractions, the good times, and the encouragement to work hard inbetween.

Contents

Declaration	i
Abstract	ii
Acknowledgements	iv
Nomenclature	xi
1 Introduction	1
1.1 Objectives	1
1.2 Assumptions	2
1.3 Sources of Information	2
1.4 Limitations of Research	2
1.5 Plan of Development	3
2 Embedded System Design using FPGA Technology	4
2.1 Introduction to FPGAs	4
2.2 ASIC vs FPGA as a design choice	6
2.3 Parallel Processing	6
2.4 System-On-a-Chip Design	7
2.5 Fast Reconfigurability	8
3 Ultrasound Tomography	10
3.1 Overview	10
3.2 Time-Of-Flight Theory	10
3.3 Ultrasound Transducers	11
3.4 Tomographical Ring Configuration	12
4 Defining the Hardware/Software Configuration	13
4.1 Objectives	13
4.2 System Overview	14

4.3	Hardware Breakdown	16
4.3.1	Mechanical Structure	16
4.3.2	Transducer Interface	16
4.3.3	MUX/DEMUX	16
4.3.4	Amplifiers	17
4.3.5	Digital-to-Analogue Converter	17
4.3.6	Analogue-to-Digital Converter	17
4.3.7	Logical Interface	17
4.3.8	Soft-core Processor	17
4.3.9	DSP Hardware	17
4.4	Software Breakdown	17
4.4.1	Control Software	18
4.4.2	Data Repository	18
4.4.3	Digital Signal Processing	18
4.4.4	Graphing Tools	18
5	Hardware Implementation	19
5.1	Sensory Equipment	19
5.2	Mechanical Stand	20
5.3	Peripheral Board - Signal Generation Circuit	20
5.3.1	Digital to Analogue Converter	20
5.3.2	Amplifier	21
5.3.3	Demultiplexer	22
5.4	Peripheral Board - Signal Capture Circuit	22
5.4.1	Programmable Gain Amplifier	22
5.4.2	Analogue to Digital Converter	23
5.5	Peripheral Board - Power Supplies	23
5.6	Peripheral Board - Voltage Shifters	23
5.7	Peripheral Board - Board Fabrication	24
5.8	FPGA Kit and Peripheral Board Interface	24
5.9	Nios II Evaluation Kit	26
5.10	Nios II Soft-core Processor & Peripherals	26
5.10.1	Overview	26
5.10.2	Configuration using SoPC Builder	27
5.10.3	PIO Interface	28
5.10.4	SPI Interface	28
5.10.5	Cyclone Pin-out Interface	29

6	Software Implementation	31
6.1	Hardware Abstraction Layer	31
6.2	Control Code	32
6.2.1	Overview	32
6.2.2	Synthesized Sine Wave Generation	35
6.2.3	Wave Capture	35
6.3	GDB Server	36
6.4	Data Processing in Matlab	37
6.4.1	Finding the TOF Value	37
6.4.2	TOF Example Set	39
7	Test Results	43
8	Conclusions	49
9	Recommendations and Proposals	50
A	Peripheral Board Schematic	52
B	Peripheral Board Assembly	54
C	Software Source Code	56
D	Matlab Functions	61
D.1	readBin.m	61
D.2	extractSampling.m	61
D.3	findTOF.m	62
E	Photograph of the final system	63
	Bibliography	64

List of Figures

2.1	An FPGA logic element, <i>courtesy of</i> [1]	4
2.2	Structure of a Xilinx XC4000 FPGA, <i>courtesy of</i> [4]	5
2.3	An example of FPGA parallelism	7
2.4	A System-on-a-chip configuration using an FPGA with on-chip RAM	8
3.1	Simple demonstration of the TOF effect	11
3.2	Tomographical Ring Configuration, showing the flight paths between transducers	12
4.1	Conceptualized System Overview	15
5.1	A transducer and its connector	19
5.2	Photographs of transducer array structure	20
5.3	Schematic of Signal Generation Circuit	21
5.4	Schematic of Signal Generation Circuit	22
5.5	Schematic of the Voltage Regulators	23
5.6	The assembled peripheral board	25
5.7	Nios II Evaluation Kit Interfaced with the custom made peripheral board	25
5.8	Basic Layout of Nios II Evaluation Kit, <i>courtesy of</i> [13]	26
5.9	Configuration of the Nios II processor and it's peripherals	27
5.10	The Nios II HDL block configured with the corresponding pins	28
5.11	Cyclone 1C12 Functional Pin-out, <i>courtesy of</i> [13]	30
6.1	The HAL fitted into the project software model	32
6.2	Flow chart of main control software	33
6.3	Flow chart of scanning algorithm	34
6.4	Pseudo code for generating a sine wave table	35
6.5	Generated sin wave values ready for transmission	36
6.6	Overview of procedure used to extract TOF values	38
6.7	Original Sample Signal	40
6.8	Sample set in the frequency domain	40

6.9	Sample set in frequency domain with zero-ed DC and negative frequencies	40
6.10	Sample set envelope	41
6.11	Sample set envelope with smoothing applied	41
6.12	Sample set with threshold and TOF determined	42
7.1	The numbering applied to the transducer transmitter/receiver pairs. (each number corresponds to a transmitter and a receiver)	43
7.2	Photograph of Red Bottle under test scenario	44
7.3	Photograph of Wooden Pole under test scenario	44
7.4	Test Subject: Empty space - raw sampled signals	45
7.5	Test Subject: Red Bottle - raw sampled signals	46
7.6	Test Subject: Wooden Pole - raw sampled signals	46
7.7	Test Subject: Empty space - surface plot of TOF values	47
7.8	Test Subject: Red Bottle - surface plot of TOF values	47
7.9	Test Subject: Wooden Pole - surface plot of TOF values	48
9.1	Proposed signal generation and DSP core configuration	51

List of Tables

2.1	ASIC Devices vs. FPGA Devices	6
5.1	DAC904 Specifications	20
5.2	ADS802 Specifications	23
5.3	The different PIO cores and their functions	29

Nomenclature

ADC—Analogue to Digital Converter

AI—Artificial Intelligence

ALU—Arithmetic Logic Unit

ASIC—Application Specific Intergrated Circuit

CAD—Computer Aided Design

DAC—Digital to Analogue Converter

DSP—Digital Signal Processing

footprint—the size or area or amount of memory/chip space that a component takes up.

FPGA—Field Programmable Gate Array

GDB—GNU Debugger

HDL—Hardware Description Layer

IDE—Intergrated Development Environment, a set of graphical user interface tools that allow the developing of code, along with debugging and version control.

JTAG—Joint Task Action Group, a standard specifying a mechanism to test and debug embedded systems and intergrated circuits

LUT—Look-Up Table

Matlab—A numerical computing environment that consists of tools for manipulating and visualizing data.

NRE—Non-Recurring Engineering, generally refers to the once-off development work for a product or system.

PGA—Programmable Gain Amplifier

RAM—Random Access Memory

SoC—System-On-a-Chip

SoPC—System-on-a-Programmable-Chip

TOF—Time Of Flight

Chapter 1

Introduction

This thesis describes the research work, design and the implementation of a FPGA-based Data Acquisition system. The application for this system is Ultrasound Tomography, however the purpose of the project was to gain an understanding of FPGA technology and implement a data acquisition system that would form a foundation for further research and practice into this form of embedded system design. Therefore, this thesis does not focus on the theory or practical nature of acoustic tomography but rather on the rapid development of a high speed data acquisition engine using relatively cheap FPGA based tools. Such a system has far reaching uses in other fields besides tomography, such as software radio, radar, image processing and any other application that relies on specific, high speed, mobile processing capabilities.

In order to fully understand the functionality of FPGA technology, this thesis takes a look at the aspects of this rapidly accelerating area of electronics. The bulk of the thesis describes the process of designing and building a data acquisition system to perform basic ultrasound scanning. Whilst this project does indeed demonstrate the speed at which systems can be implemented and tested using FPGA devices, it does not fully exploit the processing capabilities of the device. It is the natural goal of this system to allow real-time digital signal processing to take place, and this is left for further investigation and research in the future.

1.1 Objectives

The objectives of this thesis are the following:

- To provide a literature review of embedded system design using FPGA technology
- To provide a short introduction into ultrasound tomography
- To describe in detail the configuration of a data acquisition system for ultrasound tomography

- To present the results from testing the system.
- To draw conclusions on the results and suggest future improvements and extensions

1.2 Assumptions

This project covers a wide range of content that involves various fields, including systems engineering, software design, circuit design in CAD, component assembly, digital signal processing and acoustics. Thus, in order to not get overly verbose in the discussion of what has been accomplished, this thesis report assumes that the reader has an understanding of all of the above fields.

1.3 Sources of Information

The bulk of the information acquired in this project was obtained from Internet sources. Please see the in-text numbered references and the corresponding bibliography. Any other information contained here was obtained from discussions with those mentioned in the acknowledgements.

1.4 Limitations of Research

This scope of the project was limited mainly by the lack of:

- an FPGA development kit
 - An evaluation version was used instead which has intentionally limited and restricted functionality.
- licenses
 - for IP/TCP code for the kit's on-board ethernet hardware (which would have extended the project, had there been time)
- time
 - for further exploiting the capabilities of the FPGA device using digital signal processing, and to fine tune the implemented system.

1.5 Plan of Development

The following chapters in this thesis are divided up as follows:

- Chapter 2 surveys the concept of designing embedded systems using FPGA technology and the benefits it can bring to processing power and general development.
- Chapter 3 discusses the basics of ultrasound tomography and describes a sensor configuration that is used later in the implementation.
- Chapter 4 defines the hardware and software requirements for building an ultrasound tomography scanner using a FPGA device.
- Chapter 5 describes the final implementation of all the hardware related components of the system.
- Chapter 6 describes the final implementation of all the software related components of the system.
- Chapter 7 presents the results produced by the implemented ultrasound system after testing it.
- Chapter 8 discusses the results in light of the work done and draws conclusions about the implemented system.
- Chapter 9 provides proposals for project extensions and future work on the same or similar topics.

Chapter 2

Embedded System Design using FPGA Technology

This chapter provides a brief literature review of the past, present and future of FPGA technology. The purpose of understanding the basics of FPGAs is to acquire a better appreciation of the benefits that they bring to embedded systems design.

2.1 Introduction to FPGAs

FPGA is the acronym for *Field-Programmable Gate Array*. The term is most commonly applied to electronic devices which contain an array of identical logic elements which can be configured using a programming procedure to replicate any particular logic circuit. A normal FPGA device is usually contained within a single silicon package which may also house some form of memory elements[1]. A normal FPGA contains upwards of one thousand of these logic elements.

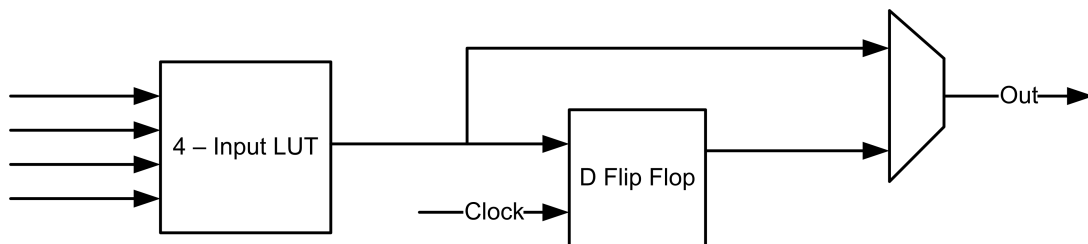


Figure 2.1: An FPGA logic element, *courtesy of* [1]

As shown by the example in figure 2.1, a logic element has a programmable Look-Up Table and a register (the flip-flop). The LUT can perform any logic function on the available inputs to produce a single logic output. The final output is either this new value or the previous value (stored in the flip-flop). Although the logic element may have more than the four inputs shown here, they generally only have one output. Figure 2.2 demonstrates the way in which logic blocks are laid out to form an array inside the FPGA. Different

Manufacturers will have slightly different configurations but all use some type of programmable switch matrix at the crossing point of the logic block interconnection lines. By having programmable switches and programmable logic elements, the system can be

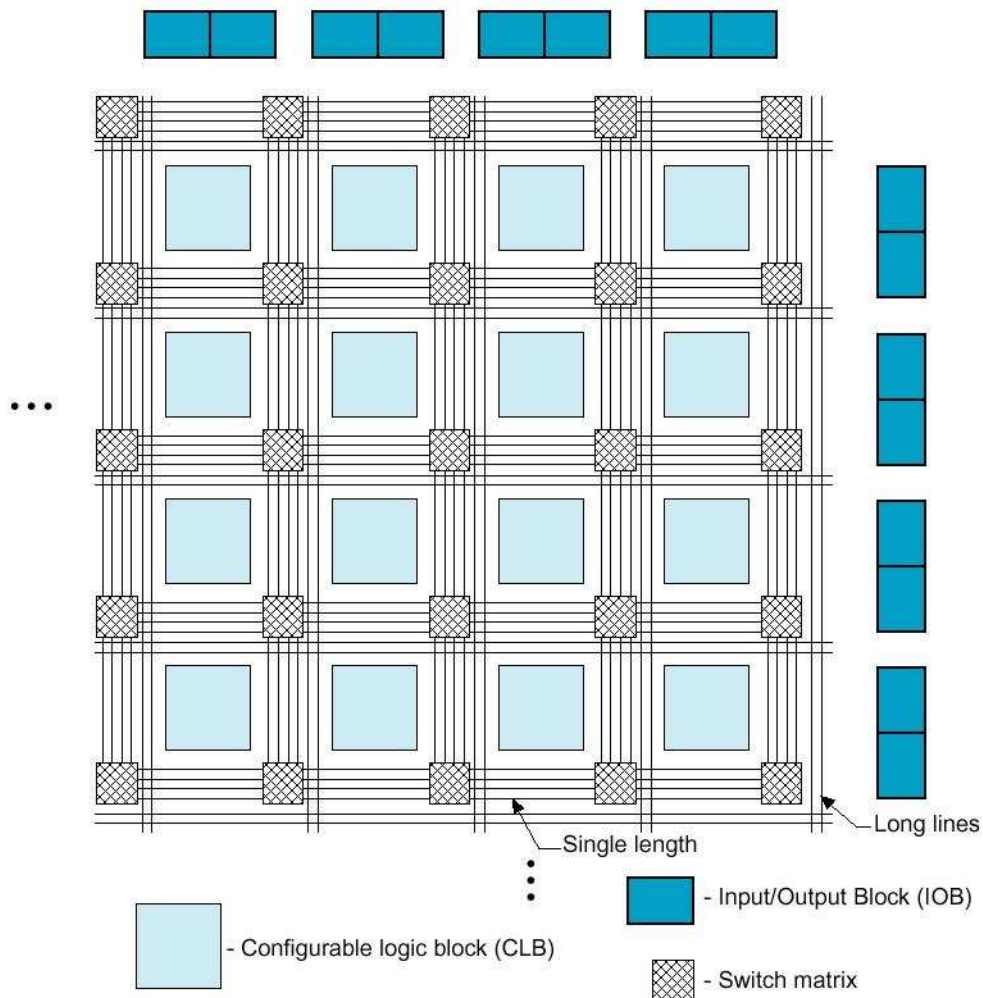


Figure 2.2: Structure of a Xilinx XC4000 FPGA, *courtesy of* [4]

configured to mimic any combination of logic functions as long as the overall design can be fitted into the available number of logic elements and switches. The process of routing a logic function into the FPGA is, of course, a highly complex process which is usually specially carried out by proprietary CAD tools designed specifically for a manufacturer's FPGA device. In general these tools allow HDL code to be imported and represented as functional blocks which are then schematically joined together and logically linked to the device's I/O pins. A hardware image is then compiled and produced using advanced AI placement routines. These routines take into account the propagational effects of line length, as well as hardware footprint and the compilation process can generally be fine tuned to the needs of the designer. This can be useful when weighing up design time vs required system footprint/speed, as a smaller faster image will take much longer to compile, delaying the design process.

2.2 ASIC vs FPGA as a design choice

ASIC technology (*Application-Specific Integrated Circuit*) has enjoyed much success in the past owing to its ability to allow for customized, high speed, efficient circuitry. The process of designing, testing and setting up fabrication facilities for the production of an ASIC is generally very expensive. In situations where the market for a certain device is large and reprogrammability is not needed, this high non-recurring engineering (NRE) cost can be countered by the smaller, faster and cheaper end product that ASIC technology produces. Strictly speaking, a working FPGA device programmed with a hardware image is in fact a type of ASIC, however the FPGA's reprogrammability makes it very different as a design choice. The advantages and disadvantages of both types of technology are summed up in table 2.1

	ASIC	FPGA
NRE Cost	High	Low
Unit Cost	Less Expensive	More Expensive
Speed	Faster	Slower
Re-Configurable in the field	No	Yes
Footprint	Smaller	Larger
Time to Market	Longer	Shorter
Cost of Debugging	High	Low

Table 2.1: ASIC Devices vs. FPGA Devices

2.3 Parallel Processing

Of the many advantages that FPGA devices offer, the ability to allow for customized parallel processing is perhaps the most beneficial of all. Since a designer no longer needs to rely on a ASIC vendor to provide him with the processing tools that he needs, the designer can quickly create his own processing blocks in hardware. This is hugely beneficial for computationally strenuous tasks, and since the cost of trial and error designing is now essentially nil, the designer is free to experiment with different processing configurations to fine tune his system. The basic concept is demonstrated in figure 2.3. The figure shows how an FPGA can be used to quadruple the speed of digital processing using an existing HDL defined DSP core, along with a control core. For a moment, let us assume that the original DSP core can perform a given operation in 4 clock cycles. This gives an output of $1/4 = 0.25$ operations per clock cycle. In the configuration in figure 2.3, the control core switches the data input and outputs in a rotational fashion thereby allowing a new input value to be applied to the inputs of a different DSP core every clock cycle. Thus the DSP blocks will operate in parallel on a single sequential stream of incoming data. Our resulting performance is $4/4 = 1$ Operations per clock cycle - a 4 fold increase. This

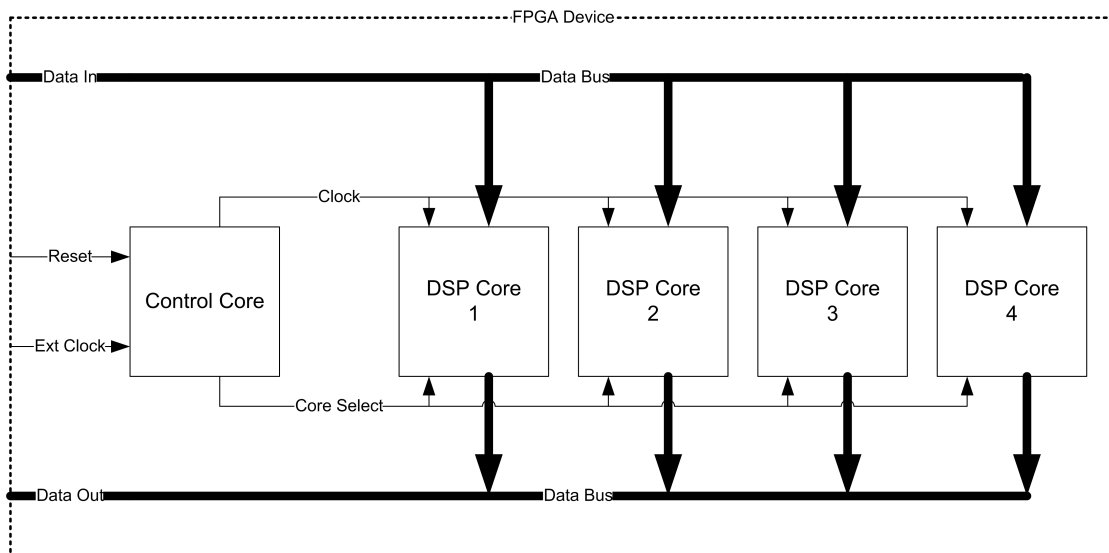


Figure 2.3: An example of FPGA parallelism

example would be fairly easy to accomplish using the appropriate CAD, and HDL-to-programmable logic tools. The DSP core would be defined in HDL code (in most cases someone else's intellectual property). The HDL code would be imported into the CAD system, along with a custom created control core (also in HDL), and these block components could be linked up logically using the graphical CAD tools. Once this is done, the whole system would be compiled into a programmable hardware image to be loaded onto the FPGA.

Note that there are many other existing ways of exploiting an FPGA to allow parallel processing. The end result in all cases is greater processing performance.

2.4 System-On-a-Chip Design

SOC devices generally include as many of a target system's resources on one chip as possible. This includes analogue functions, digital functions, logic converters, I/O interfaces, memory banks and even radio-frequency functions on a single package[5]. Although this makes designing a SOC quite a difficult task, the benefits over using separate components are a smaller, faster, more power efficient and much more reliable system.

Most modern FPGAs will incorporate a form of memory structure which is separate from the array of logic elements which make up the programmable logic. Because it is contained within the chip, this memory is fast relative to external RAM and thus provides a cache storage function for systems which contain a micro-processor. This makes FPGAs perfect for fast SOC design. Generally these cache areas are very small and will hold 1000 bits or more of information. Figure 2.4 demonstrates the structure of an FPGA that has on-chip RAM.

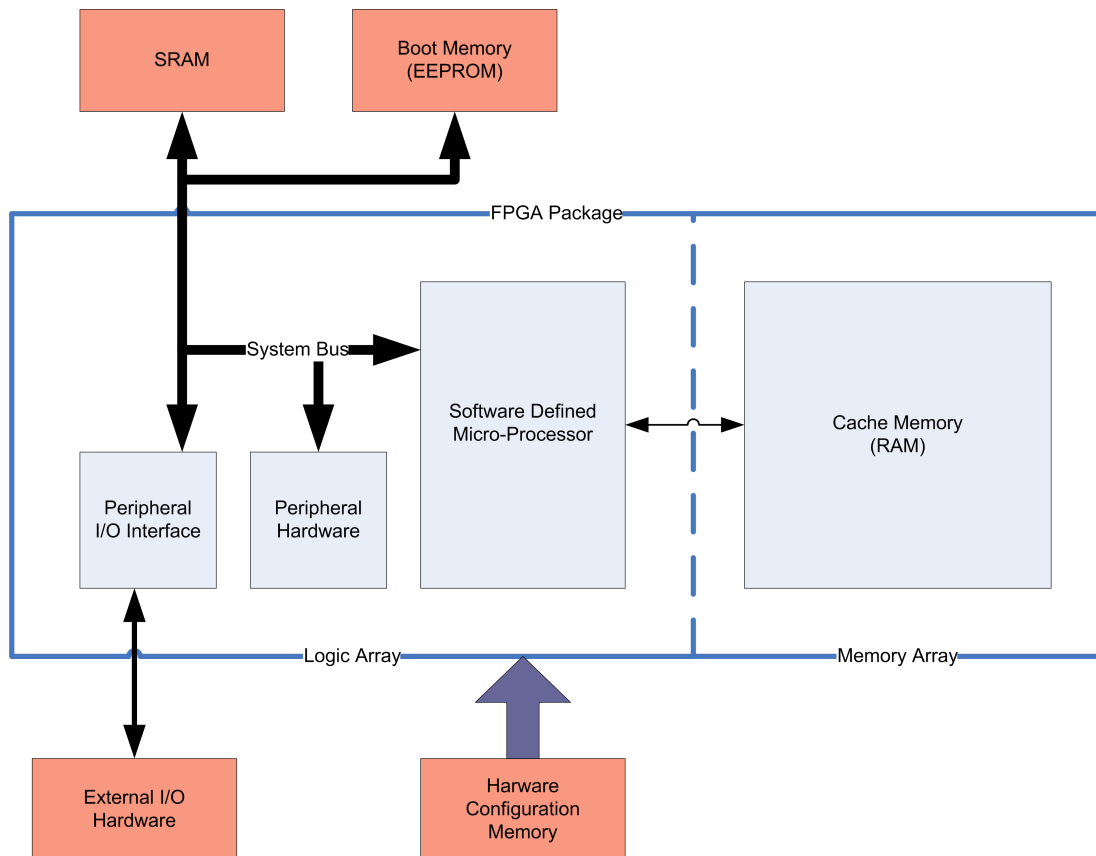


Figure 2.4: A System-on-a-chip configuration using an FPGA with on-chip RAM

The example SOC in figure 2.4 has all its vital components included on the FPGA. Since an FPGA will lose its stored hardware image as well as its data storage when the power is switched off, the SOC must be facilitated by either a flash or EEPROM equivalent device to store the original hardware image, as well as any software that must be booted. Generally the hardware image is stored in a serial EEPROM device which automatically loads itself into the FPGA upon reset.

2.5 Fast Reconfigurability

Besides their inherent parallelism, the other outstanding benefit of FPGA technology is the ability to be reprogrammed in the field of operation. This makes them an attractive design choice for device manufacturers who expect to have to supply updates to their product. In such a case, the permanent memory device supporting the FPGA is flashed with the new hardware image, along with any new software. A good example of this is the TV Set-Top-Box manufacturers who are currently designing new decoder systems[6]. Their systems need to cope with the new MPEG-4 video streams and still have the ability to switch over and decode old MPEG-2 video streams. This can be accomplished by configuring the FPGA device with a controller which automatically reprograms the FPGA with the appropriate hardware image depending on the data stream to be processed.

Reconfigurability also drastically reduces the development time-cycle allowing products

to be produced quicker and ultimately cheaper.

Chapter 3

Ultrasound Tomography

This chapter describes the basic theory behind ultrasound tomography. Since the project takes a very simplistic approach to tomography and deals mainly with the basic principles of acoustic time-of-flight, the mathematics for tomographical reconstruction and acoustic wave theory are beyond the scope of this project. Thus this chapter is necessarily brief and merely touches on this large field of knowledge. The following information was mainly gathered from reading [7], which delves into this topic with much more detail.

3.1 Overview

Sound is a propagating mechanical effect. It can occur in all matter where molecules are close enough to allow a mechanical disturbance to travel through that matter as a wave. These waves can be described by their amplitude, frequency, wave length, phase and speed[9]. Ultrasound merely refers to sound waves that have a frequency above that which the human ear is capable of hearing. Ultrasound has a multitude of applications in the biomedical and industrial fields but has also been deployed in weaponry and range-finding.

One industrial application of ultrasound is to non-invasively find flaws in materials. Ultrasound waves are transmitted into an object, and then the resulting waveforms are captured from different points in space around the target. Sometimes, the reflected wave is captured instead, in which case the wave is captured from the same point in space. By analyzing the received waves, measuring particular characteristics of these waves and then applying special mathematical formulae to the resulting data, an image of the target can be constructed.

3.2 Time-Of-Flight Theory

Since the speed of a sound wave depends on the medium in which it is traveling, different types of material will effect the propagation of a generated sound wave. This phenomenon

can be exploited by transmitting ultrasound waves through a target object from various different points in space, and measuring the resulting waves from other points in space around the target.

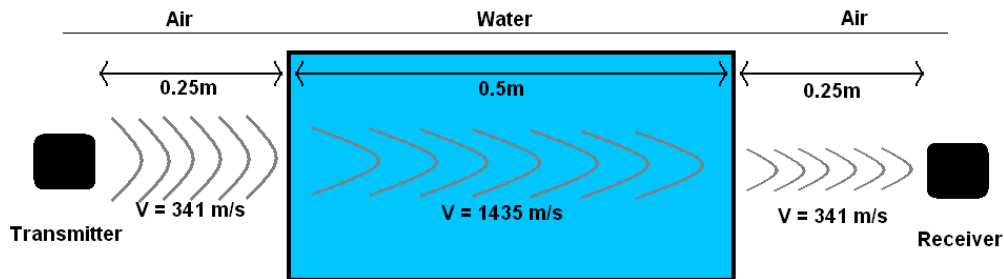


Figure 3.1: Simple demonstration of the TOF effect

In figure 3.1, the effect of medium on propagation speed is demonstrated. The speed of sound in air at sea level is approximately 341 m/s, whilst the speed of sound in water is approximately 1435 m/s. Although temperature and pressure play a role in propagation, if we assume that these are constant, they can be neglected to aid simplicity. If we consider the distances in figure 3.1, it can be seen that the time for a sound wave to travel to the receiver would be:

$$t = \text{metres} / \text{metres per second} = 0.25/341 + 0.5/1435 + 0.25/341 = 0.0018 \text{ s}$$

Now consider the same calculation with the tub of water removed, so that the two transducers have line of sight through only air:

$$t = \text{metres} / \text{metres per second} = 1/341 = 0.0029 \text{ s}$$

From this it can be seen that the speed of propagation is a characteristic of a sound wave that can yield information about the medium it travels through. This measurement is called the time-of-flight value, abbreviated as TOF.

3.3 Ultrasound Transducers

In order to generate or capture an ultrasound wave, a form of transducer is needed to interface the electronics with the outside world. Ultrasound transducers are cheap, widely available products that operate in the ultrasound frequency range.

Particular types of transducers will have different characteristics based primarily on their frequency response. Transducers generally are bandpass filters since they are only responsive or receptive to a narrow frequency band[2]. In this project, as will be seen later, the transducers that were available were air-coupled piezoelectric 40 KHZ devices. This means they were only responsive to the frequency band centered on 40 KHZ. In practice this was found to be closer to 40.5 KHZ.

3.4 Tomographical Ring Configuration

As stated in section 3.2, to find various TOF values, it is necessary to transmit and receive ultrasound waves through various points in space around a target object. A logical configuration for gathering TOF information for a 2D cross-section of a target object is the ring formation. In the ring formation, illustrated in figure 3.2, an array of transducers are placed at constant spaces around the circumference of a circle, the radius of which would be determined by the size of the target object. It can be shown that the symmetry of this formation lends itself to producing TOF values that are mathematically friendly for modeling the makeup of a target object within the circle[7].

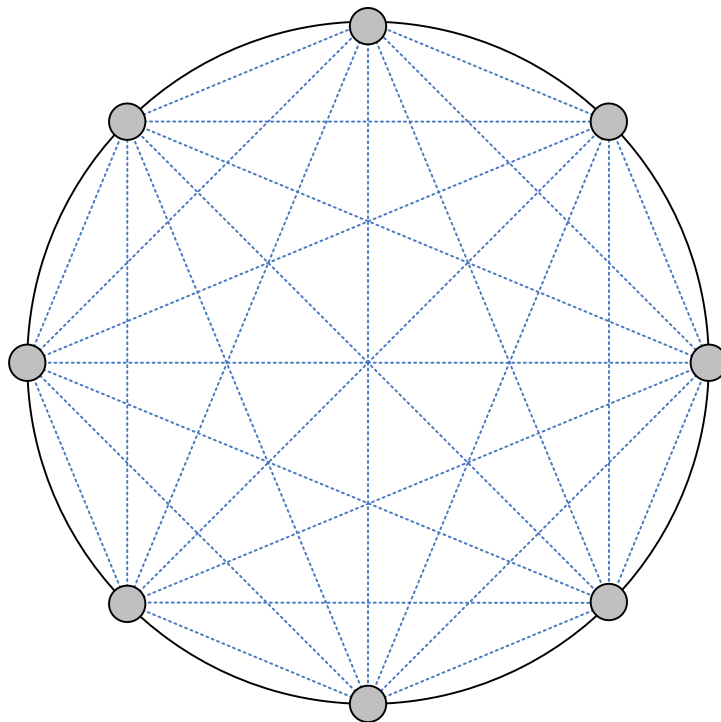


Figure 3.2: Tomographical Ring Configuration, showing the flight paths between transducers

Chapter 4

Defining the Hardware/Software Configuration

This chapter details the planning process of an FPGA-Based Data Acquisition system. It describes how:

- the main functional requirements were identified
- the system configuration was brain-stormed
- the main components were identified
- all the component interfaces were identified

4.1 Objectives

In order to accomplish simple ultrasound tomography, the system had to meet the following goals:

- Array of transducers
 - House an array of transducers in a ring formation around the target object, as described in section 3.4.
- Sound wave generation:
 - Digitally generate any type of ultrasonic wave
 - Convert this wave into its corresponding analogue signal
 - Amplify the signal to an appropriate level
 - Transmit the wave on any one of the array of transducers
 - Pass this wave through the target object

- Sound wave capture:
 - Receive the resulting wave on any one of the transducers
 - Sample the wave at a speed greater than ten times its Nyquist limit frequency[2], but preferably as fast as possible.
- Switching
 - Allow the transmission and capturing to occur in rapid succession between different transducers
- Data Analysis
 - Using knowledge of the transmitted and captured waveforms, extract the TOF values and create a visual representation of the extracted data

4.2 System Overview

By examining the system requirements in section 4.1, a basic configuration concept was developed (see figure 4.1).

The configuration was heavily influenced by the resources available at the time of design:

- Transducers
 - The devices available at the time of development were separate transmitter receivers, which meant one set of transmitters and one set of receivers were needed. These would be overlay-ed to simulate the transmitter/receiver pairs being in the same point in space. See section 5.2 for more details. It was decided that 8 transducer pairs would be enough to give some valuable results[2].
- Peripheral Board
 - A PCB manufacturing machine was available for use at UCT, thus the entire collection of peripheral devices could be built onto one board. Since this was a prototype project, sample surface mount chip packages could be sourced from international chip manufacturers and delivered, all for free. Resistors and capacitors could be purchased at a local component distributor.
- FPGA Kit

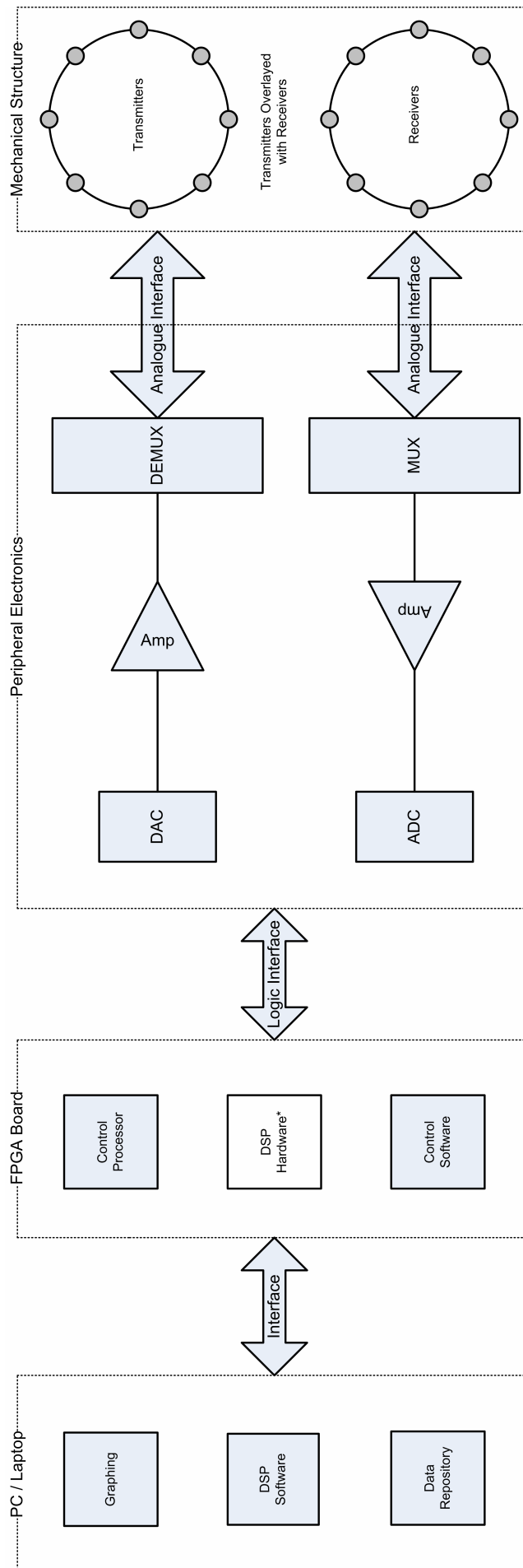


Figure 4.1: Conceptualized System Overview

- An Altera Nios II Evaluation Kit was available to use. The evaluation kit comes with an entry level Cyclone FPGA device, 16MB SRAM, as well as a JTAG interface. Most importantly, the Evaluation Kit comes with all the necessary software for creating custom hardware images for the FPGA. The kit includes a customizable soft-core processor (NIOS II), CAD and HDL compilers, as well as an Integrated Development Environment (IDE) for creating software to be downloaded and executed on the FPGA.
- Personal Computer
 - A PC was available on which the development tools could operate.
- Matlab
 - A copy of Matlab was available. Matlab is a powerful set of numerical data-manipulation tools incorporated with graphing and other visualization facilities. This was ideal for extracting the results from the raw data.

4.3 Hardware Breakdown

The breakdown of following hardware requirements is illustrated by the system block diagram in figure 4.1.

4.3.1 Mechanical Structure

A mechanical structure was needed to house the array of transmitters and receivers. Since the transducers used were air-coupled devices, and thus would not be stuck directly onto the target object, the structure had to offer low sound reflection. Thus there could not be any flat surfaces in the vicinity of the transducers. The structure also had to have a means of easily placing a target object into the array of transducers.

4.3.2 Transducer Interface

The transducers needed to be individually connected to the peripheral board. This would be an analogue interface with each transducer having a pair of wires running back to the peripheral controlling board.

4.3.3 MUX/DEMUX

A demultiplexer was needed to select which transducer channel to transmit on at any given time. A multiplexer was needed to select which transducer channel to receive on at any given time. During the scanning process, the channels could be switched in a rotational fashion to collect samples for the flight path between every receiver and every transmitter.

4.3.4 Amplifiers

An amplifier would be needed to apply gain to the the analogue signal created by the Digital to Analogue converter. This output would then be fed into the DEMUX to channel it to the right transducer. A amplifier was also needed on the receiving end to amplify the weak signal collected from the receivers. Ideally, this receiving end amplifier needed to have a controllable gain to account for a variation in possible signal strengths.

4.3.5 Digital-to-Analogue Converter

A fast DAC was needed with a high resolution output, as well as a fast conversion time. (~ 1 Msps, >= 14 bit resolution)[2]

4.3.6 Analogue-to-Digital Converter

A fast ADC was needed to sample the received signal from the receiver amplifier. (~ 1 Msps , >= 12 bit resolution) [2]

4.3.7 Logical Interface

A cabling system would need to connect the peripheral board with the FPGA evaluation kit. There would be a multitude of logical channels so this cabling would need many parallel lines.

4.3.8 Soft-core Processor

Some sort of HDL defined processor was needed on which to run control code for the system. The processor would perform all the sampling and control the devices on the external data acquisition circuitry.

4.3.9 DSP Hardware

The ultimate reason for using an FPGA for implementing the ultrasound scanner was to allow for digital signal processing on the FPGA device. This would be left as a natural future extension for this project.

4.4 Software Breakdown

The breakdown of software requirements below is illustrated by the system block diagram in figure 4.1.

4.4.1 Control Software

Software was needed to control the operation of the peripheral hardware. The software would control the scanning procedure as well as the data capture. It would also designate what type of signal was synthesized to be generated as an analogue signal through the DAC.

4.4.2 Data Repository

Since the DSP Hardware would come later as a project extension , it would be necessary to send all raw data back to the PC and thus some sort of data repository would be needed to store the sampled data.

4.4.3 Digital Signal Processing

Since the DSP Hardware would come later as a project extension, it would be necessary to perform digital signal processing on the PC using the data in the data repository referred to in section 4.4.2.

4.4.4 Graphing Tools

In order to visualize the results of the sampling and DSP, a means of graphing and displaying the processed data was needed. Although generating a 2D cross-section representation of the target object is out of the scope of this thesis, it would be preferable to demonstrate visual information that could confirm the operation of the system.

Chapter 5

Hardware Implementation

This chapter explains how the sensors and custom peripheral board for the project were built from the ground up, and configured. It also describes how the soft-core processor and its peripheral system-on-a-chip components were built and configured, for although they were designed and built in software, they obviously acted as hardware components in the final system. This demonstrates the power of embedded system design using FPGAs.

5.1 Sensory Equipment

The transducers used were the type available from the local electronics store.

- Transmitters were of type: ST40-12SP 753S
- Receivers were of type: SR40-12SP 753S

These transducers only operate effectively on a narrow frequency band centered on 40KHz and their roll-off in sensitivity is sharp around this centre frequency. Each transducer had to be soldered to its own pair of wires, which had a simple 2-pin female connector at the other end, demonstrated in figure 5.1.

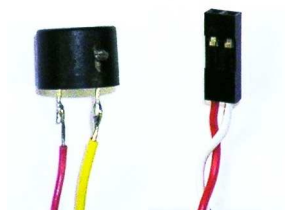


Figure 5.1: A transducer and its connector

5.2 Mechanical Stand

An ideal transducer array would be in a reflectionless arrangement so that no sound “echos” would occur. Although this is not entirely important in a Time-of-flight scenario, it was preferable not to have any bad reflections. An initial idea was to drill holes in the side of a container such as a bucket since this would offer an easy method of holding the transducers in a circular ring. However, such a method could cause bad reflections. Thus the easiest option was to build a small wooden structure with poles that could hold each pair of transmitter/receivers away from large flat surfaces (as these would cause sound reflections). Figure 5.2 shows the resulting structure.

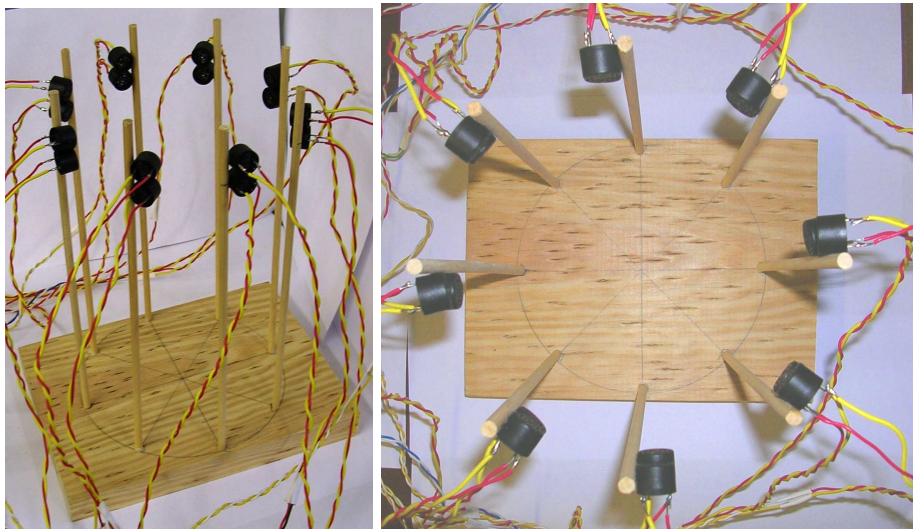


Figure 5.2: Photographs of transducer array structure

5.3 Peripheral Board - Signal Generation Circuit

5.3.1 Digital to Analogue Converter

Although the speakers used in this project were 40 KHz transducers, it was preferable to leave room for a wide range of signals to be generated. It was also preferable to allow for a high resolution control over the output voltage[2]. Thus a high specification DAC was used. Table 5.1 shows the specifications of the device. The DAC904 met the conversion

Specification	Value
Conversion Speed	165 Msps
Resolution	14 bits
Power Supply	5V or 3V
Output Type	Differential Current

Table 5.1: DAC904 Specifications

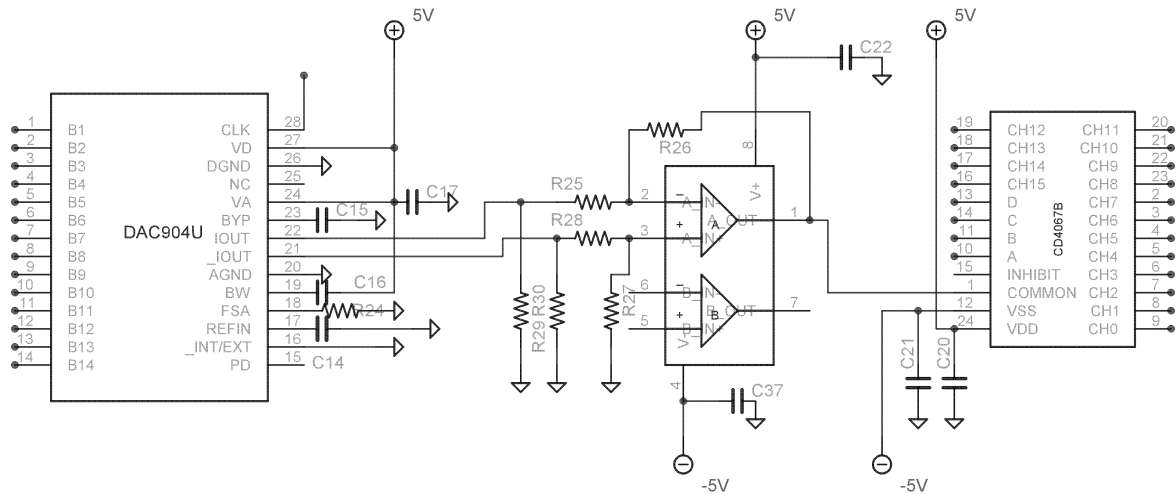


Figure 5.3: Schematic of Signal Generation Circuit

criteria specified in section 4.3.5 many times over. It was chosen merely because it gave much room to play around in, and could also be delivered quickly. Another benefit for this device is that it had all its logic input pins on one side of the device, making it much easier to lay the board out. The logic pins are shown disconnected in figure 5.3, to aid simplicity.

As can be seen from figure 5.3, the DAC is set-up in its differential current configuration according to its documentation[10]. A simple explanation of this configuration is as follows: The DAC outputs each give a full-scale output of 20mA, since the resistors(R29, R30) coupling these outputs to ground are both seen as 25Ω, this current produces a voltage of $V = 15\text{mA} * 25\Omega = 0.375\text{V}$. This full-scale voltage can then be amplified by the amplifier, which is configured with a gain of 10, giving a resulting output range of +/- 3.75V.

5.3.2 Amplifier

The amplifier to be used to amplify the analogue output signal had to meet some strict criteria in terms of its small signal frequency gain response. Once again, this was merely to leave room for various types of signals to be generated. The amplifier selected was the OPA2822 operational amplifier. With a gain configuration of 10, its small signal frequency gain response drops to -3dB at roughly 15MHz, more than ample for the application. This op-amp had two channels of which only one was needed, as can be seen in figure 5.3. The operational circuit was designed according to the recommended specifications in [10], allowing a differential output from the output of the DAC to be converted to a amplified single output signal. The op-amp was powered by +/-5V supplies. These allowed for a output voltage to swing comfortably between 4.5V and -4.5V, enough to generate a reasonably powerful signal across the terminals of a transducer. Section 5.3.1 shows, however, that the resulting full scale output signal was +/- 3.75V

5.3.3 Demultiplexer

The CD4067B is an analogue 1 to 16 demultiplexer which has typically a 125Ω loss across it. It was a -3dB bandwidth of 14 MHz, and since it is powered by a \pm supply passes a signal centered on zero. Figure 5.3 does not show the output enable and output selection logic lines connected up. These allowed control over the selection of the output channel.

5.4 Peripheral Board - Signal Capture Circuit

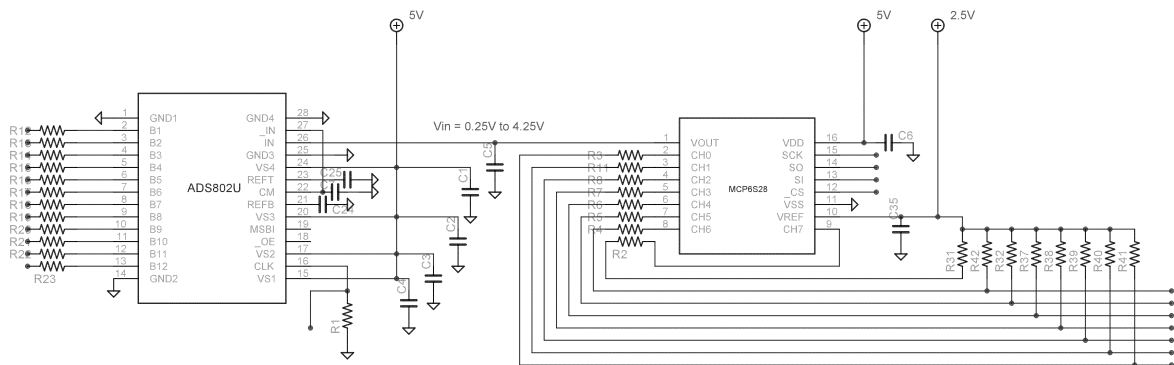


Figure 5.4: Schematic of Signal Generation Circuit

5.4.1 Programmable Gain Amplifier

Programmable gain amplifiers allow the gain of the amplifier to be controllable using digital logic. In this case, a Microchip MCP6S28 device was used. It had the benefit of having digitally controlled gain as well as multiple possible input channels (8 channels). This made the device ideal for this application. Effectively it meant the device could act as a amplifier and multiplexer all in one. It's only limiting capability was that it's maximum gain setting had a -3dB bandwidth value of 2 MHz. However, this was still adequate for the application. The PGA was supplied with 3 voltages, a positive supply at 5V, base reference at ground and a 2.25V reference at VREF. By setting VREF at 2.25 V, this allowed the output signal to be centered on 2.25V as required by the ADC (see section 5.4.2).

Since the amplifier was operating between 0 and 5 Volts, it was desirable to have the input signals centered on 2.25V, thus each input channel was voltage shifted by the same 2.25V reference, as can be seen on the right hand side of figure 5.4.

The gain and input selection of the MCP6S28 is controlled by a Serial Peripheral Interface (SPI). This is described in greater detail in section 5.10.4.

5.4.2 Analogue to Digital Converter

The Texas Instruments ADS802 was the device used to sample the analogue signal at high speed. Its specifications are listed in table 5.2. The analogue input/s could be configured in either a differential or single input configuration, but the device was configured in the single input configuration for simplicity[12]. This means that it had a full scale input range of 0.25V to 4.25V. Since the ADC offered a 12 bit resolution, it offered output values ranging from $(2^0 - 1) = 0$ to $(2^{12} - 1) = 4095$. Therefore a voltage at 2.25V would register $\frac{4095}{2} = 2047$ as a sampled value.

Specification	Value
Sampling Rate	10 MHz
Resolution	12 bits
Power Supply	5
Output Type	5V logic

Table 5.2: ADS802 Specifications

5.5 Peripheral Board - Power Supplies

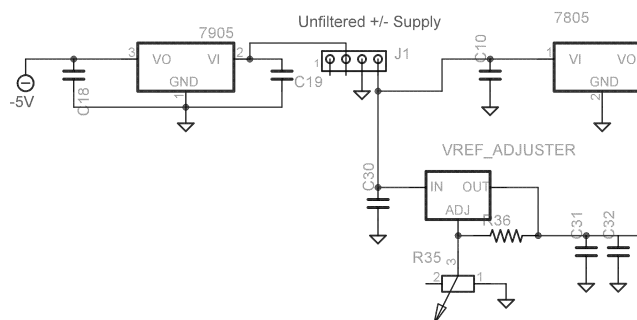


Figure 5.5: Schematic of the Voltage Regulators

The various components on the peripheral board were powered by 3 different voltage regulators, a -5V Supply (L7905), a 5V supply(L7805) and a 2.25V reference voltage supply (LM317). The inputs and outputs of the regulators were filtered by placing the recommended capacitor values according to their respective data-sheets. The layout of the regulators can be seen in figure 5.5. In practice, surface mount capacitors were not adequate for this purpose, and these were replaced with leaded tantalum capacitors.

5.6 Peripheral Board - Voltage Shifters

Since the FPGA kit used 3.3V logic levels, and the components on the peripheral board used 5V levels, there had to be some means of level shifting the logic signals between the

peripheral board and the FPGA kit. This was accomplished by using M74HCT541 Octal Non-Inverting buffer devices where needed. The 5V voltages originating at the ADC were simply current limited by placing 2K resistors on each logic line, thereby protecting the FPGA pins from high current load and bypassing the need for a return 5V-to-3.3V shifter. This configuration can be seen in the final schematic in the appendix A.

5.7 Peripheral Board - Board Fabrication

The schematics and assembly for the peripheral board were done in Eagle CAD. The resulting PCB was printed using UCT's recently purchased fast prototyping machine. The process involves placing a protective film over the blank copper-silicon-copper plate, drilling the through holes and vias, then applying solder paste to couple the vias. Once this was done, the film was removed and the plate was placed in an oven for 30 minutes to set the solder paste. The plate was then placed back into the prototyping machine for its tracks to be etched out of the copper, and the periphery of the board to be cut from the rest of the plate, leaving the remaining plate reusable.

The components used on the board were all obtained using sample requests from the respective chip manufacturers. Passive surface mount components were bought in reels from a local distributor. The process of soldering was tedious, but resulted in a very functional board, which suffered from relatively few problems. As stated in section 5.5, some leaded tantalum capacitors were used instead of the surface mount ones, as they proved to provide better decoupling for the power supplies. Initially there was a misconception about part of the data-sheet for the programmable gain amplifier, and an additional power supply was used unnecessarily. This was removed and the board was patched. The voltage level shifting of the incoming signals from 0V to 2.25V as stated in section 5.4.1, was actually done after the fabrication process by soldering the extra 2K resistors standing up vertically and then soldering a wire bridge across these resistors connecting them with the 2.25V supply (see bottom right area of figure 5.6).

5.8 FPGA Kit and Peripheral Board Interface

There were a large number of logic channels that needed to be connected between the peripheral board and the FPGA kit. Figure 5.7 demonstrates how this was accomplished using normal parallel IDE cable. The pins on the peripheral board were laid out according to the channel they would match up with on the kit prototyping pins. These were then easily connected using the cables and some pin headers on either side.

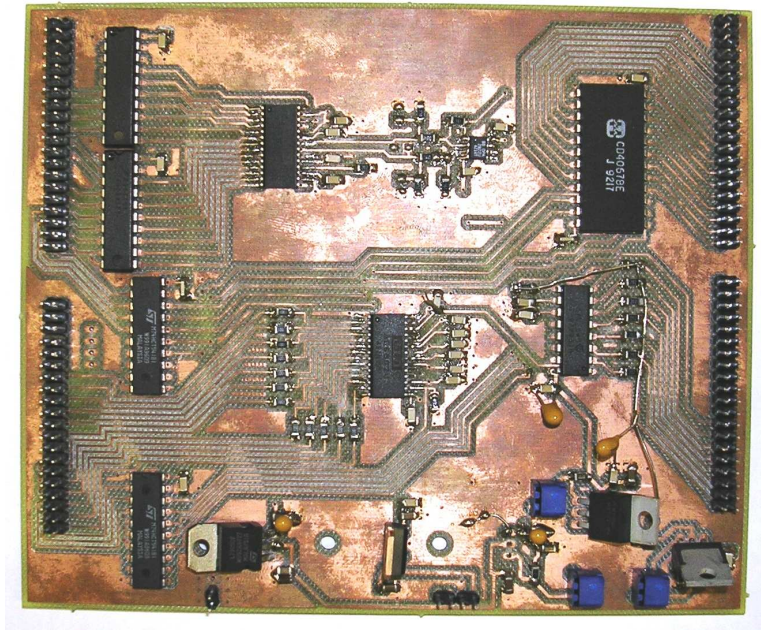


Figure 5.6: The assembled peripheral board

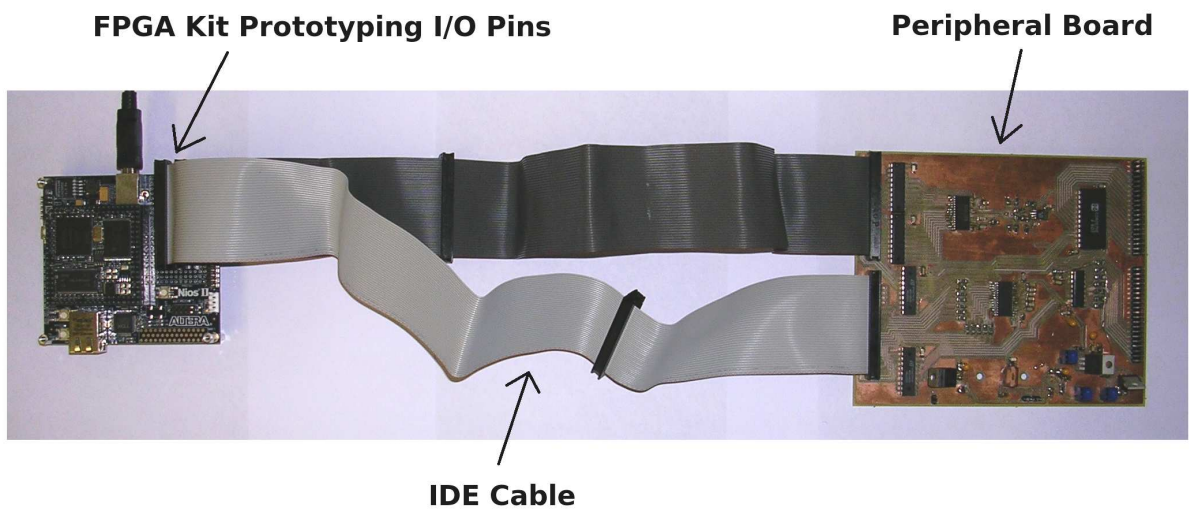


Figure 5.7: Nios II Evaluation Kit Interfaced with the custom made peripheral board

5.9 Nios II Evaluation Kit

The platform on which the processing capabilities of this system were built, and on which future work will be done, was the Altera Nios II Evaluation Kit. The kit is meant to be an evaluation board for the Nios II soft-core processor, although it can be used for any purpose for which it meets the requirements. It is composed of a FPGA device (the Altera Cyclone FPGA), and accompanying crystal oscillators, voltage regulators and standard interfaces (JTAG, Serial, Ethernet and straight logic prototyping pins). The basic layout is as shown in figure 5.8. This kit comes with all the tools necessary to develop programmable images for the FPGA device, as well as an IDE to create software for the Nios II soft-core processor.

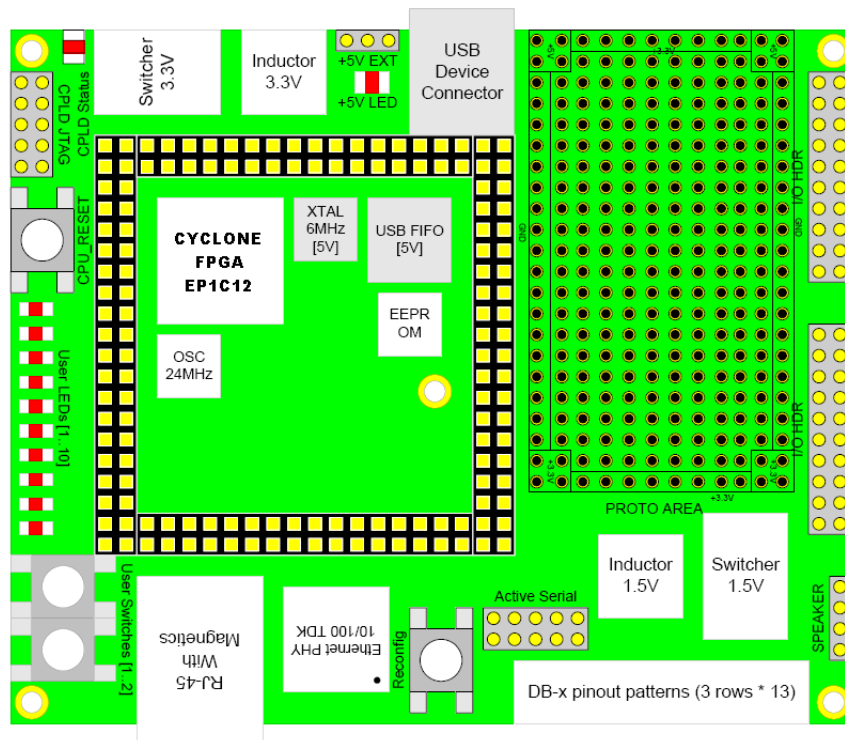


Figure 5.8: Basic Layout of Nios II Evaluation Kit, *courtesy of* [13]

5.10 Nios II Soft-core Processor & Peripherals

5.10.1 Overview

The Nios II is a 32-bit embedded software defined processor that is almost entirely configurable, providing a best-fit configuration for any application. Since it is software defined, the Nios II can be modified by adding or removing various peripheral components, as well as choosing which type of Nios II core to use based on desired core attributes:

Fast with Large Footprint

Standard with Medium Footprint

Economy with Small Footprint

The **Fast** has the fastest performance (measured in Dhrystone MIPS), and the largest logic footprint, whilst the **Economy** has the slowest performance but with the smallest logic footprint. The advantage of the software defined nature of the Nios II is that custom instructions can be placed alongside existing instructions in the ALU of the processor. This allows designers to tweak the performance of the processor for their application. The processor also comes complete with a standardized Avalon Bus to allow it to communicate with embedded peripherals and even additional software-defined processors[14]. Figure 5.9 demonstrates how the processor and it's peripheral embedded components where configured. For this project, the Nios II was implemented with a **Fast** core and with the extra peripherals shown in the figure.

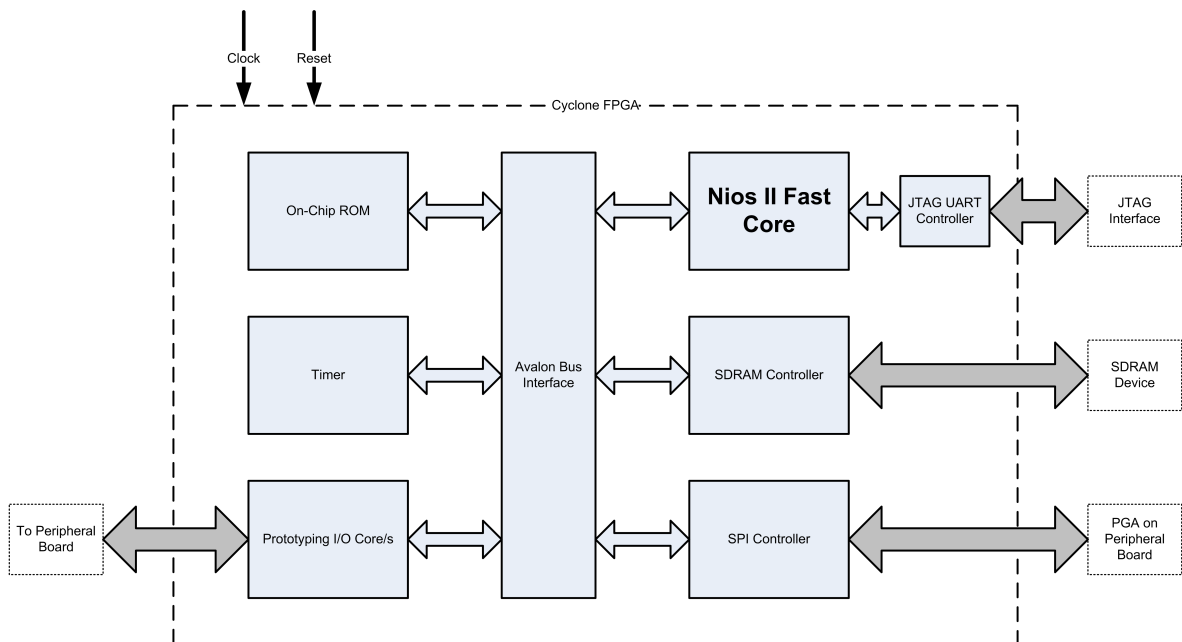


Figure 5.9: Configuration of the Nios II processor and it's peripherals

5.10.2 Configuration using SoPC Builder

SoPC Builder (System-on-programmable-Chips) allows the basic Nios II processor to be customized by configuring it's core size, cache sizes, custom instructions and also it's peripheral components and interfaces. The SoPC builder produces a single HDL block which contains the core processor, the Avalon Bus (see figure 5.9) and all peripheral cores. This block is then imported into the Quartus CAD software to be interfaced with the other custom on-board components, and to allow it to be connected to external FPGA pins. Figure 5.10 shows the customized Nios II processor block built for this project using SoPC builder and imported into the Quartus CAD environment. External pins are shown

PIO Core	Function
<i>ADC_clk</i>	To interface with the ADC's clock pin
<i>ADC_in</i>	To interface with the ADC's 12 output pins
<i>DAC_clk</i>	To interface with the DAC's clock pin
<i>DAC_out</i>	To interface with the DAC's 14 input pins
<i>DEMUX_inhibit</i>	To interface with the Demultiplexor's inhibit pin
<i>DEMUX_select</i>	To interface with the Demultiplexor's channel select pins
<i>SV2</i>	To interface with the extra pins on the board (wasn't used)
<i>extra_pins</i>	Bidirectional Interface to extra pins on the peripheral board (wasn't used)

Table 5.3: The different PIO cores and their functions

the same way as the PIO Core. This SPI core accepts values to be written to the SPI device and automatically controls the transfer according to the specifications of the SPI standard (timing, bit-rate etc). It can be set as a slave or master device and handle multiple other devices on the same interface, however in this case it was implemented as a master SPI device controlling a single slave device (the PGA). The SPI interface appears in figure 5.10 as the segment 2nd from the bottom.

5.10.5 Cyclone Pin-out Interface

The bottom of the Cyclone 1C12 FPGA device is an array of pin connectors that is mapped out by figure 5.11. The pads on which the cyclone is soldered are hardwired to individual pins on the prototyping area of the Nios II Evaluation Kit (see right hand side of figure 5.8). The yellow blocks in figure 5.11 indicate where prototyping pins have been mapped to. This means that the hardware image created by Quartus must have it's appropriate I/O lines correctly matched with the positions in the figure. In order to do this, the pin allocation facility in Quartus was used. This allows the designer to specify a FPGA pin for every pin that appears in the CAD design (see figure 5.10).



Figure 5.11: Cyclone 1C12 Functional Pin-out, *courtesy of [13]*

Chapter 6

Software Implementation

This chapter describes how the project software was designed and created using the software tools supplied with the Nios II Evaluation Kit. The Nios II IDE is a programming environment shipped with Evaluation Kit. It automatically creates a hardware abstraction layer (see section 6.1) for a custom Nios II configuration. Application code can then be written that uses functions exported by the HAL, and during the compiling process, the drivers, HAL and application code are all linked and bundled together. The application code for this project can be seen in appendix C. The chapter also describes how the raw data was processed in Matlab to produce visual information, in order to determine if the system was working as planned, and to provide the results shown in chapter 7.

6.1 Hardware Abstraction Layer

The SoPC builder software described in section 5.10.2 automatically memory maps the additional peripheral cores into the processor's accessible memory space. This means that the processor "sees" these additional peripherals as normal memory addresses. This allows these memory address values to be assigned to variable names, so that procedures can be written to abstract away the low-level interface with peripheral components.

In fact, SoPC builder has the ability to create a HAL (Hardware Abstraction Layer) for an individual Nios II configuration and exports this as C code with associated library files. This means that all that needs to be done is to write the application code for system by using calls to the exported functions provided by the HAL. This dramatically speeds up the development time, and it is for this reason that the code here is so simple. The actual low-level hardware interfacing code has been abstracted away.

Wherever possible, this HAL exports its functions as ANSI C Standard Library function look-alikes, such as *fopen()*, *fwrite()* and *printf()*[15]. This allows the programmer to access the peripherals using standard C function calls. Obviously this is not always possible, as certain devices do not fit the Standard C model for data streams, file access etc. One example of such a device is the SPI Core. Figure 6.1, taken from [15], but modified for the project scenario, demonstrates how the HAL fits in with the software model.

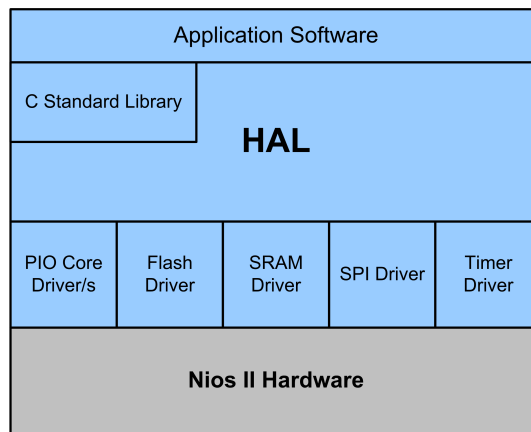


Figure 6.1: The HAL fitted into the project software model

6.2 Control Code

6.2.1 Overview

This section explains how the software which controls the ultrasound scanner works. Since the system was a prototype design and there was limited development time, the system was controlled by commands sent to the processor using the JTAG debug interface. The JTAG module was capable of performing the following functions [taken from [16]]:

- Downloading application software into the SDRAM
- Starting and stopping the program execution
- Setting breakpoints and watchpoints
- Analyzing registers and Memory
- Collecting real-time execution trace data
- Interfacing the program with a GDB server (see section 6.3)

Now , even though the JTAG module would potentially slow the processor down by placing breakpoints in the code, it was possible to use only a stripped down version of the JTAG module which only allowed for a serial interface with the PC, and allowed for breakpoints to be ignored. It was noted that this had no effect on the speed at which the processor ran, even though the JTAG serial interface is very slow. Only when a data stream was written or read from the JTAG interface was there a reduction in speed. This allowed the whole scanning process to be controlled via a JTAG serial interface. The application software was extremely basic and allowed a user to set the required gain, and to instruct the system to perform a scan. The algorithm for program control is represented

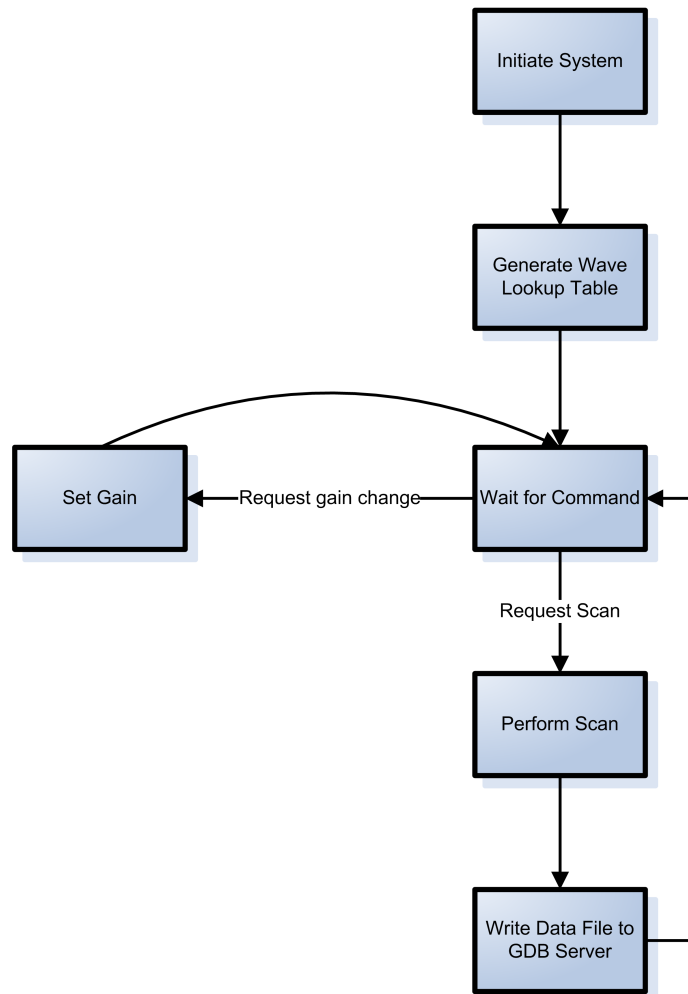


Figure 6.2: Flow chart of main control software

by the flow chart in figure 6.2, whilst figure 6.3 shows the flow chart for performing a scan.

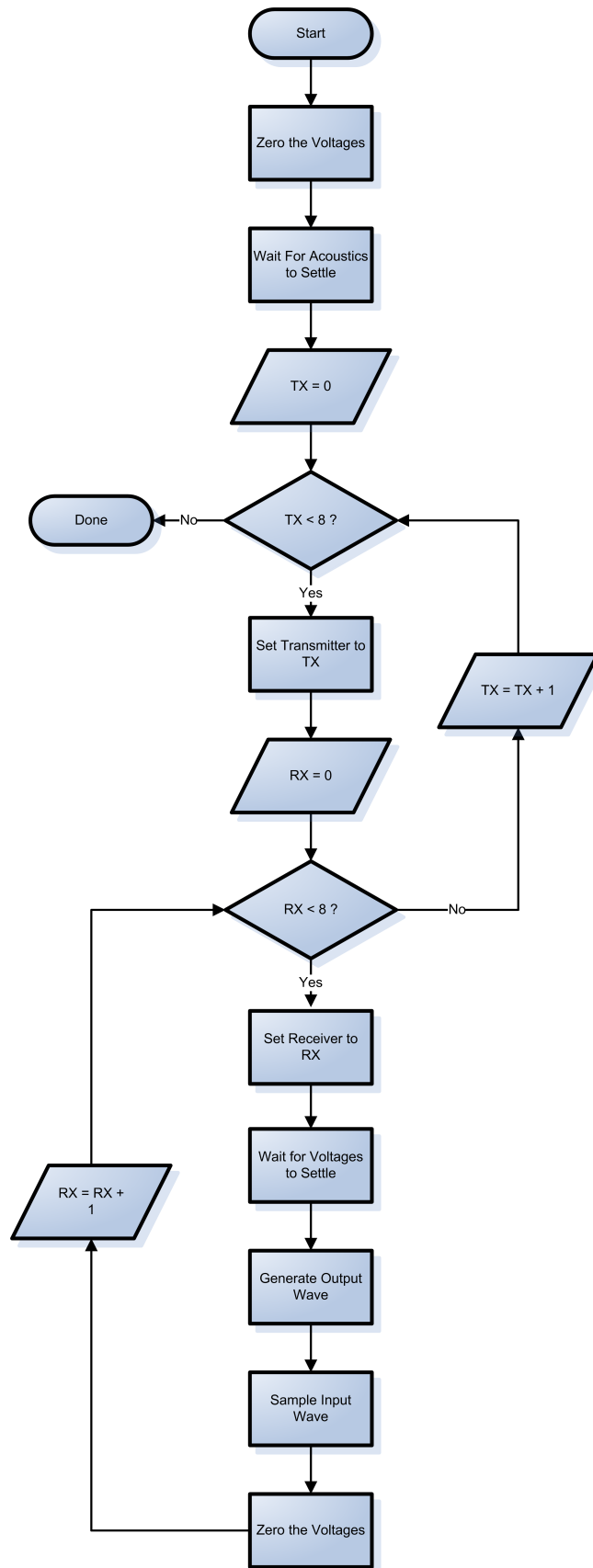


Figure 6.3: Flow chart of scanning algorithm

6.2.2 Synthesized Sine Wave Generation

In order to generate a basic 40 KHz sine wave to be transmitted as a test signal, it was necessary to have knowledge of the sampling speed capabilities of the processor. When certain hardware is programmed into the FPGA, the Quartus auto-routing software makes estimates of the latency of certain instructions, but these can only be confirmed by testing the final design.

In order to determine at what speed the processor could spit out data values to the DAC, a simple test program was created. This application essentially had a loop that read a value from memory, sent this value to the DAC, and then toggled the DAC clock. This loop ran repeatedly and the voltage on the clock line was analyzed using an oscilloscope. The clocking frequency was found to be 1.267 MHz.

Figure 6.2 indicates that a wave look-up table is created after system initialization and before control is passed to the user. The sampling frequency above was using to create the sine table of sample values in memory that could be fed at a rate of 1.267 Mega-samples-per-second to the DAC. The pseudo code in figure Figure 6.4 on page 35 shows how the table was filled with 100 samples of a sine wave: Here the *DAC_RES* value

```
MAX = 1266666
FREQ = 40500
DAC_RES = 16384
DELTA_T = 1 / MAX
M = DAC_RES / 2
FOR (I = 1 TO 100) LOOP
    TABLE[I] = SIN(2*PI*FREQ*DELTA_T*I) * M + M
    TABLE[I] = ROUND_OFF(TABLE[I])
END LOOP
```

Figure 6.4: Pseudo code for generating a sine wave table

is the decimal resolution of the DAC, which in this case is a full scale range of $2^{14}=16384$ different possible values. In other words, after reviewing section 5.3.1, a value of 0 applied to the DAC will give an output voltage of -3.75V and a value of 16384 will give a full-scale voltage at +3.75V. Figure 6.5 demonstrates what the generated wave of 100 samples would look like. Note how the last value is not zeroed, but this is not important as the output voltage is returned to zero by stabilizing the voltages (see figure 6.3)

6.2.3 Wave Capture

The same test was done for reading in values from the ADC. A loop was run that first clocked the ADC, read a value from the output lines of the ADC, then wrote the integer value into memory. The oscilloscope showed that the result was exactly the same as when reading from memory, 1.267 MHz. This effectively meant that the expected 40.5KHz ultrasound wave, could be sampled at 1.267 MHz, or over 31 times its own Nyquist limit.

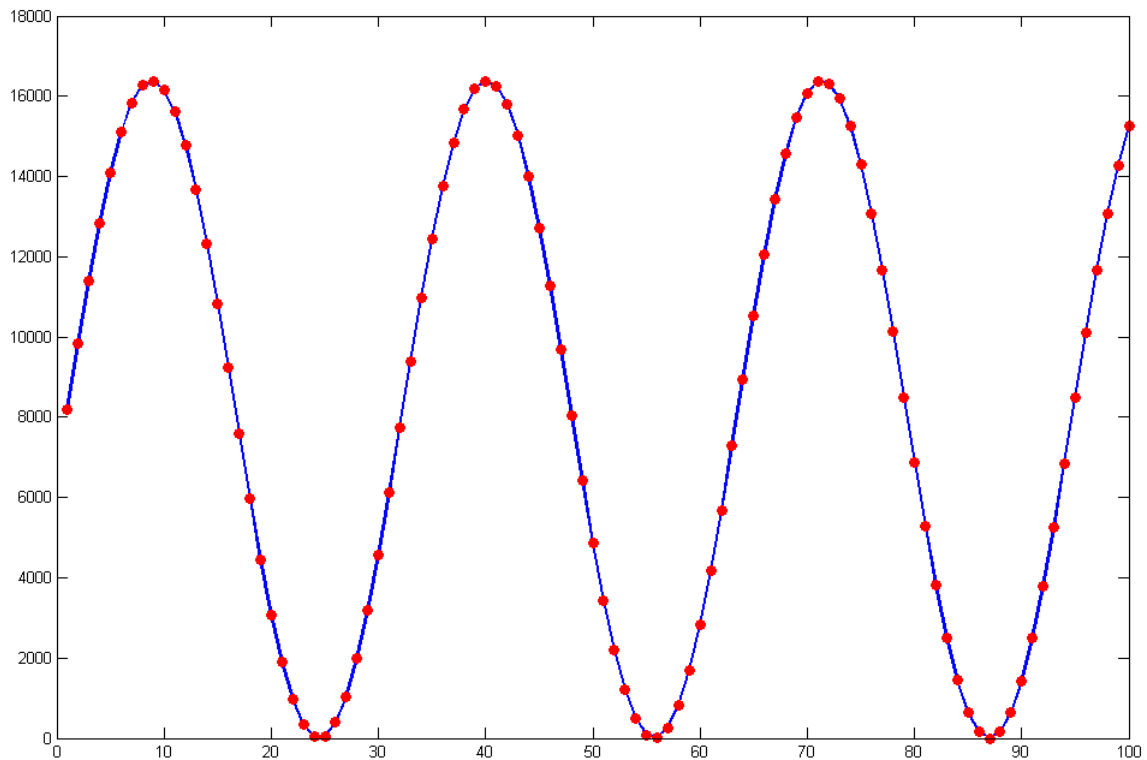


Figure 6.5: Generated sin wave values ready for transmission

This would give a very accurate representation of the resultant wave. The process of sampling a resultant wave was simple. For sampling, simply begin clocking the ADC at 1.267 MHz when the transmitted wave was finished being sent, (as show in figure 6.3) and in between clock cycles, read off the value on the output of the ADC. The captured sample should have a brief time of no activity and then as the first sound pulse arrives at the receiver, a sudden rise of values. We are interested only in the time of this first pulse, as explained in section 3.2. A sampling size of 1000 was decided upon, as a sufficient size sampling to catch the incident wave in it's entirety, even for the longest trajectory. The whole set of values captured by the scanning process depicted in figure 6.3 would therefore be 8 transmitters * 8 receivers * 1000 samples = 64,000 samples. If each sample occupied 2 bytes in memory (16 bits) this would give a total memory requirement of $2 * 64,000 / 1024 = 125$ KBytes, an amount easily matched by the Evaluation Kit's 16 MB of SDRAM.

6.3 GDB Server

Section 4.4.2 called for a data repository were the wave capturing system could permanently store the raw sampled data retrieved using the scanning process. Since the system was being operated via a JTAG interface (an interface meant for debugging) it was convenient to make use of a GDB server facility. GDB stands for GNU Debugger, and it

provides a means for the application running on the Nios II processor to be able to write a file on the remote PC just as if it was writing to its own local file-system. This process is still limited by the speed of the JTAG interface, but is much more efficient than sending the data back on the JTAG command shell interface as ASCII text. By executing the application through the Nios II IDE with a GDB server enabled, the target application could write a binary file on the host machine. Thus as long as the SDRAM on the FPGA kit was big enough to hold one set of sampled values, the system had a fail-safe data repository.

In order to send the files back to the host PC, the standard C file handling procedures were used. This included using file pointers, and the *fwrite()* command. The data was written by sequentially writing the 12 bit samples, packaged as 16 bit binary values, to the opened file. This created a file size of 125 KBytes, as demonstrated at the end of section 6.2.3. The file was then opened in Matlab to perform some signal processing, which is explained in the next section.

6.4 Data Processing in Matlab

6.4.1 Finding the TOF Value

Once the raw data was held as a binary file, it could be opened using Matlab and analyzed. The purpose of this processing was to extract the Time-of-flight (TOF) information from the raw data and graph this information so that the system's validity could be verified. Figure 6.6 demonstrates the procedure followed to produce TOF information from the raw data. In order to prepare the data for processing, the binary values were read into a 3-dimensional ($8 * 8 * 1000$) array. Now since the ADC produces 12 bit binary values that represent a range of 0 to 4096, centered on $4096 / 2 = 2048$, it was necessary to subtract a value of 2048 from each sample to produce values centered around zero. Then for each of the 64 of the sets of 1000 samples a common procedure was applied, and for each set a time-of-flight value was produced and placed in a 3D ($8*8*1$) array. The following list describes the reasoning behind each step shown in the flowchart (figure 6.6).

1. **Fast Fourier Transform** - To find the signal's frequency spectrum, the Matlab *fft()* function was used. This produced a set of 1000 complex numbers, and for each of these the absolute value was taken.
2. **Zero-ing the DC frequency value and values after the 500th sample** - Because of the inaccuracy of the 2.25V reference on the peripheral board, the signals weren't centered exactly on zero, therefore the DC component needed to be removed. In the discrete frequency domain, the DC component is found in the sample representing zero Hertz. This value was forced to be zero. In order to find the TOF value, only the envelope of the signal waveform was needed so that the first pulse edge can

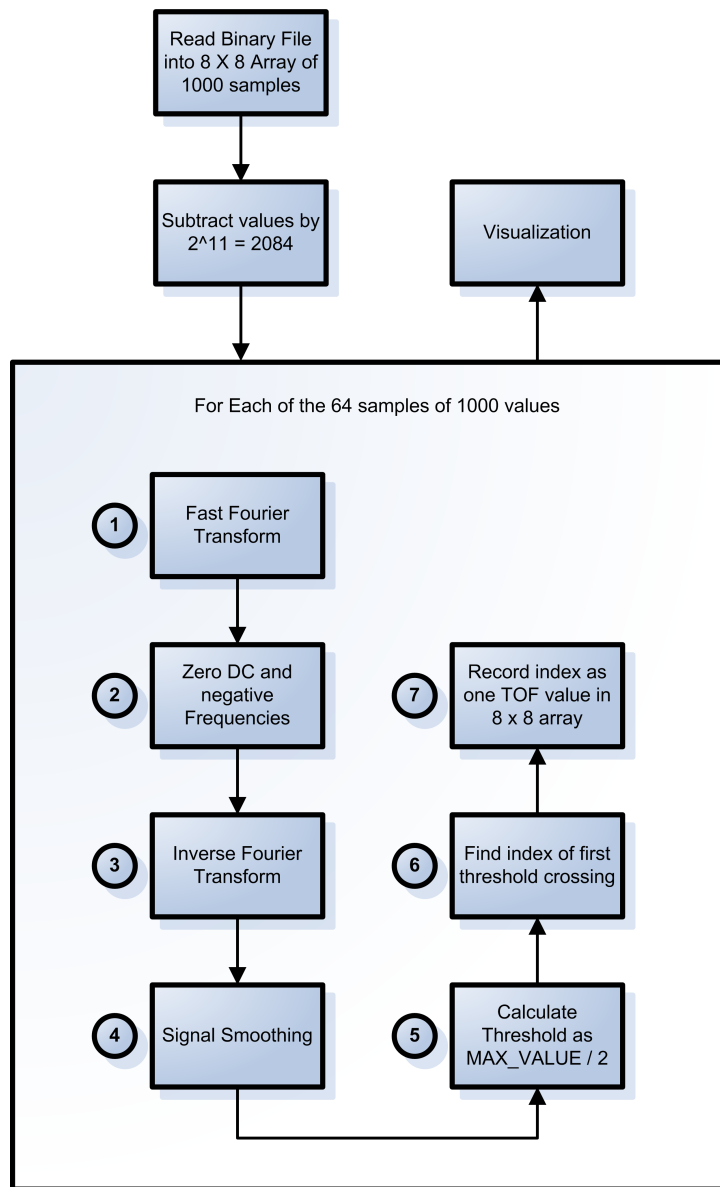


Figure 6.6: Overview of procedure used to extract TOF values

be found. The envelope was found by zero-ing all the negative frequency components (those values represented in sample 501 up to and including 1000) and then applying the *ifft()* in step 3.

3. **Inverse Fourier Transform** - The *ifft()* Matlab function was used to convert the discrete frequency domain values back into the time domain. By doing so, just the envelope of the original signal is found. Although the first rising edge could still be detected using the the original signal, the “cleaned up” envelope signal provides a better waveform from which to find the the TOF value.
4. **Signal Smoothing** - In order to further clean the waveform, the signal is smoothed using a 10-point moving average weighting (the Matlab *smooth()* function)
5. **Calculation of threshold value** - A suitable means of finding the first rising edge

(indicating the arrival of a ultrasound pulse) was found using trial and error. Most algorithms find the rising edge by looking for the index of the point where the signal first crosses a “universal” threshold value that is preset. In this case, however, a universal value was ineffective as different signal paths produced wildly different amplitudes and it was possible for the threshold to be missed completely or perhaps triggered by noise. Instead, the maximum value in the set of 1000 values was found. This value was halved, and the halved value became the threshold for that set of samples.

6. **Finding Threshold Crossing** - Once the threshold value was determined, the set of 1000 samples was searched for the index of the first value to pass the threshold value. It was necessary to ignore the first 50 samples, as sometimes spurious medium amplitude signals could be found (probably due to circuit feedback). This proved to be quite an effective way of discovering the first rising edge and therefore the TOF value.
7. **Recording Index as TOF** - Once the TOF value was found, it was recorded in its appropriate index in the $8 * 8$ array of TOF values.

6.4.2 TOF Example Set

This subsection serves to illustrate the process outlined in the previous section by visualizing the process through its various stages. It follows the process of analyzing one set of 1000 samples to find its TOF value.

- Firstly a raw set of 1000 samples was extracted from the binary file, figure 6.7 shows the extracted signal.
- Next the Fast Fourier Transform is applied to the sample set; see figure 6.8
- Next the DC component is zero-ed and the negative frequencies are also zero-ed.; see figure 6.9
- Next the sample set is Inverse-Fourier Transformed back into the time domain; see figure 6.10
- Next sample set is smoothed to remove unwanted spurious edges; see figure 6.11
- Next the maximum value is found, this value is halved and the first intersection of the result is located. This becomes the TOF value; see figure 6.12

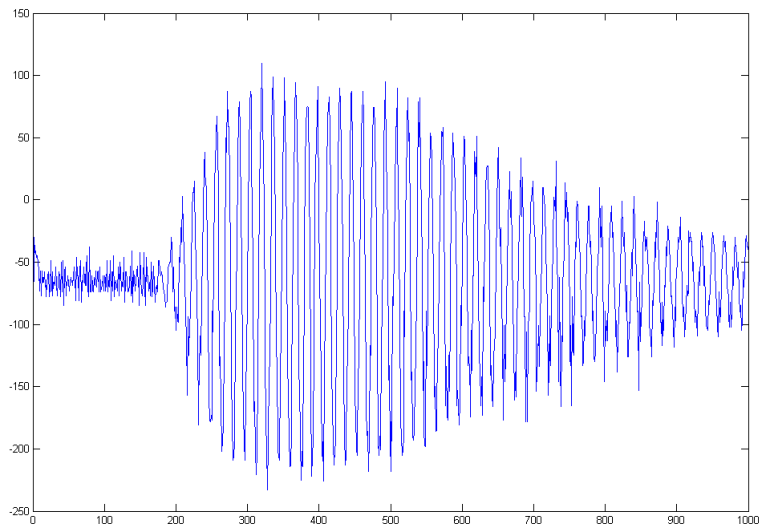


Figure 6.7: Original Sample Signal

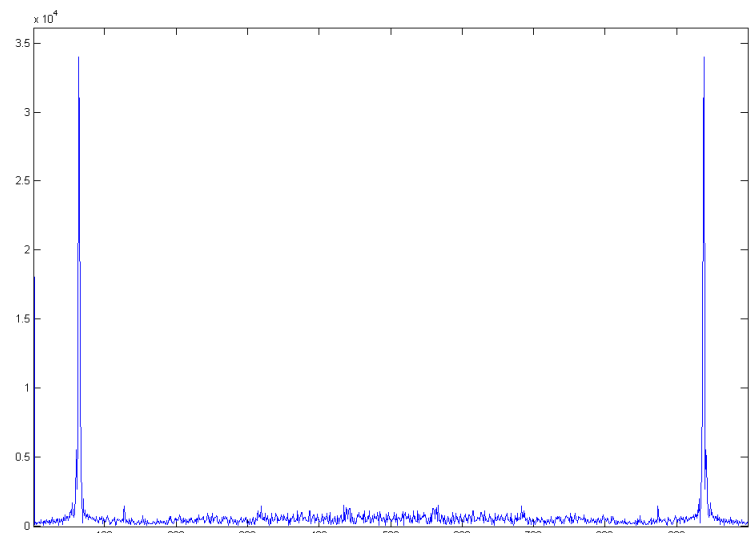


Figure 6.8: Sample set in the frequency domain

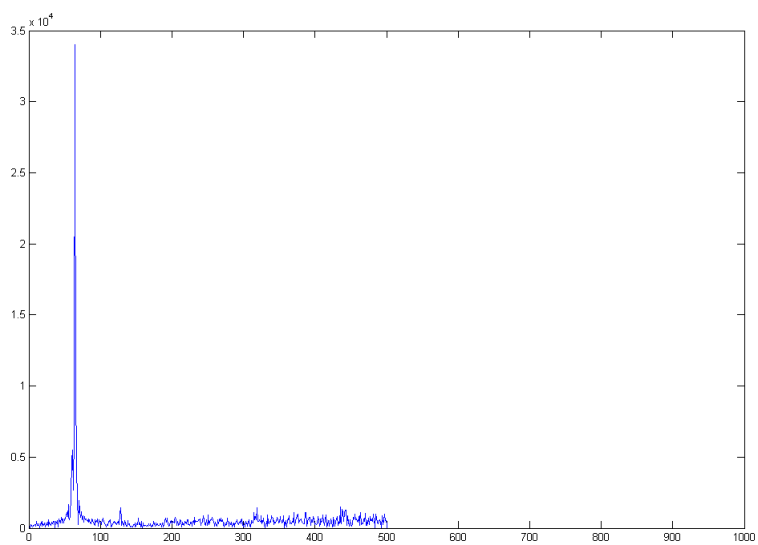


Figure 6.9: Sample set in frequency domain with zero-ed DC and negative frequencies

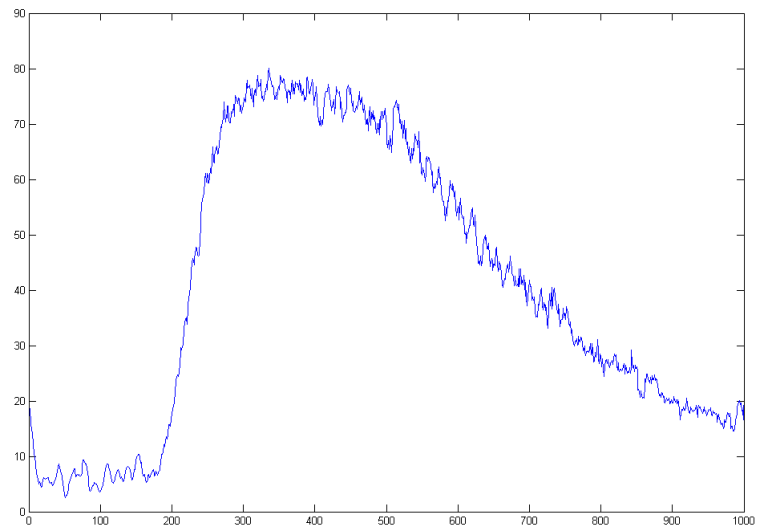


Figure 6.10: Sample set envelope

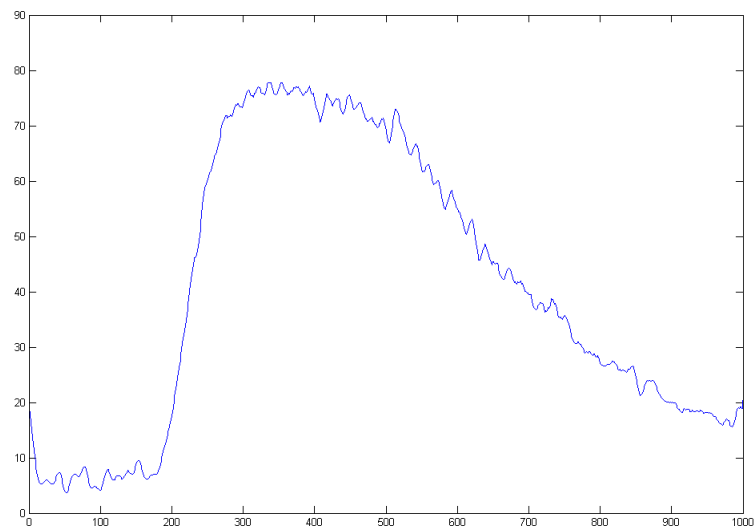


Figure 6.11: Sample set envelope with smoothing applied

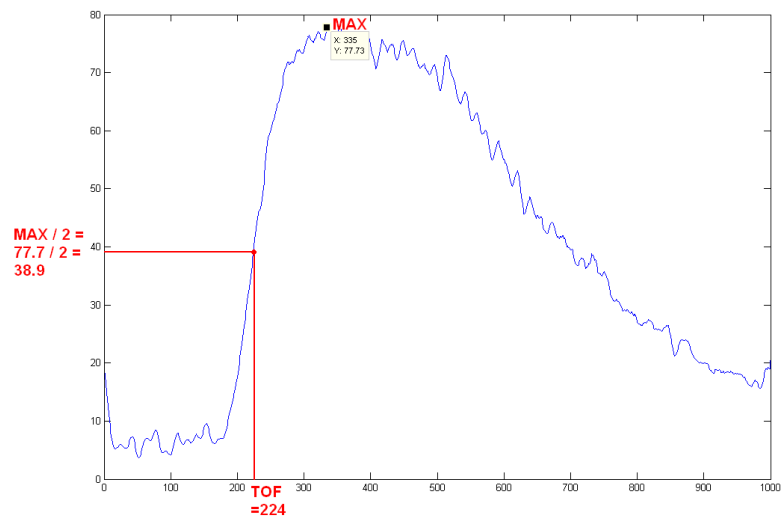


Figure 6.12: Sample set with threshold and TOF determined

Chapter 7

Test Results

In order to test the operation of the implemented system, a few target objects were selected. The first target was simply the open space between the sensors - i.e. no object was placed within the ring. This was so that further scans of actual objects could be compared with the empty scan to gauge the difference or effect that a target object has on the TOF values. Apart from the empty scan, two different objects were scanned, a hollow red bottle with a small cross-sectional area, and a length of dense wooden pole with a large cross-sectional area. Figures 7.2 to 7.9 illustrate the information obtained during these tests. Figure 7.1 shows how the transducers where numbered, this helps to interpret the TOF surface plots.

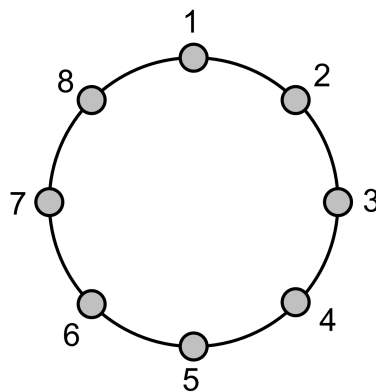


Figure 7.1: The numbering applied to the transducer transmitter/receiver pairs. (each number corresponds to a transmitter and a receiver)

The resultant TOF values indicate the the system is correctly deducing the propagation speed between different transducers. By inspecting figure 7.7 we can see that the surface plot dips low at the points that correspond to the TOF values where the transmitter and receiver where essentially in the same position and as such give the lowest TOF values. The red areas in the figure indicate flight paths that had large TOF values and these correspond to transmitter/receiver pairs that where on opposite sides of the ring formation from each other.

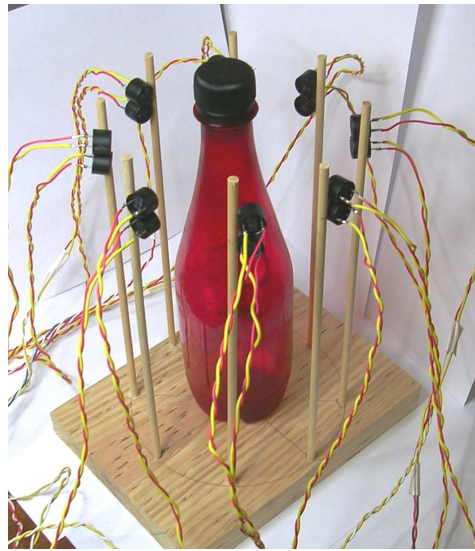


Figure 7.2: Photograph of Red Bottle under test scenario



Figure 7.3: Photograph of Wooden Pole under test scenario

Most importantly, by comparing figures 7.7 and 7.8 we can see that the red bottle has had a noticeable influence on the TOF values, indicated by the rising TOF values corresponding to flight paths that intersect the centre of the ring formation. These are paths that intersected the red bottle neck and would thus be effected by its presence.

Figures 7.6 and 7.9 show how when the wooden pole was scanned, it seemed the ultrasound waves did not penetrate the wood at all. This was probably due to the transmitted signals lack of power (a peak-to-peak amplitude of 7.5 V) or perhaps the fact the fact that the transducers where not directly coupled with the wood. The result of this was that the TOF readings for the paths that intersected the wood, were simply close to 0. This was because the receiver only picked up random noise and thus this upset the rising-edge finding process.

From all the results shown, it is obvious that the system is however, not fine tuned. For

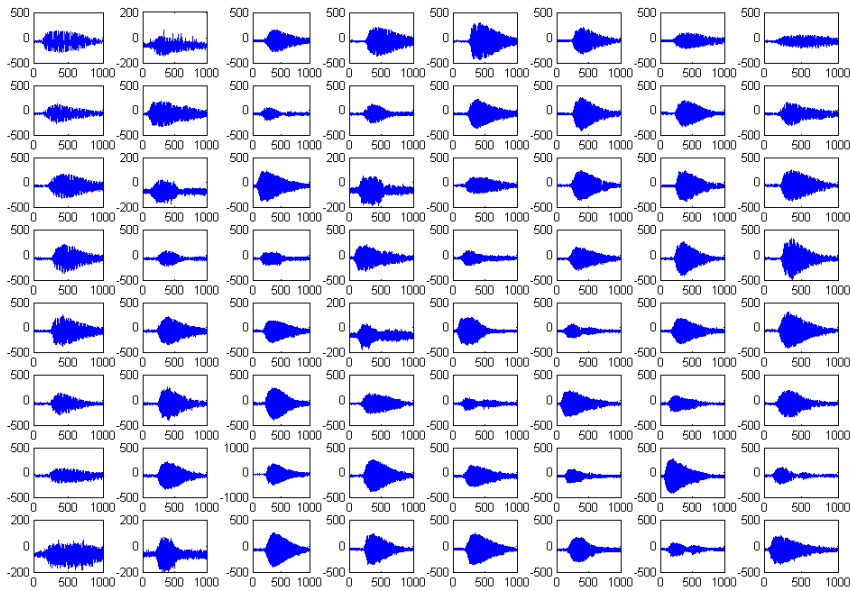


Figure 7.4: Test Subject: Empty space - raw sampled signals

example, the raw data samples in figure 7.4 are not centered precisely on zero, and they fall well within the range of -500 to 500 in value. Compare this to the resolution of the system (12 bits) and we can see the values should vary between -2048 and 2048. This indicates that the full receiver gain of 32 was inadequate, even when no target object was there to cause signal loss. It also indicates that a more powerful ultrasound signal should be generated at the transmitters, to properly penetrate the target object.

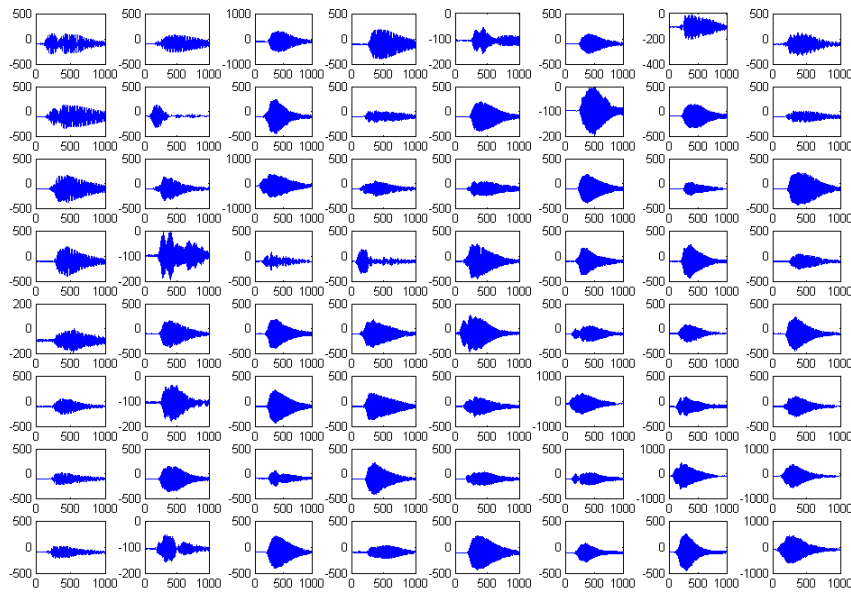


Figure 7.5: Test Subject: Red Bottle - raw sampled signals

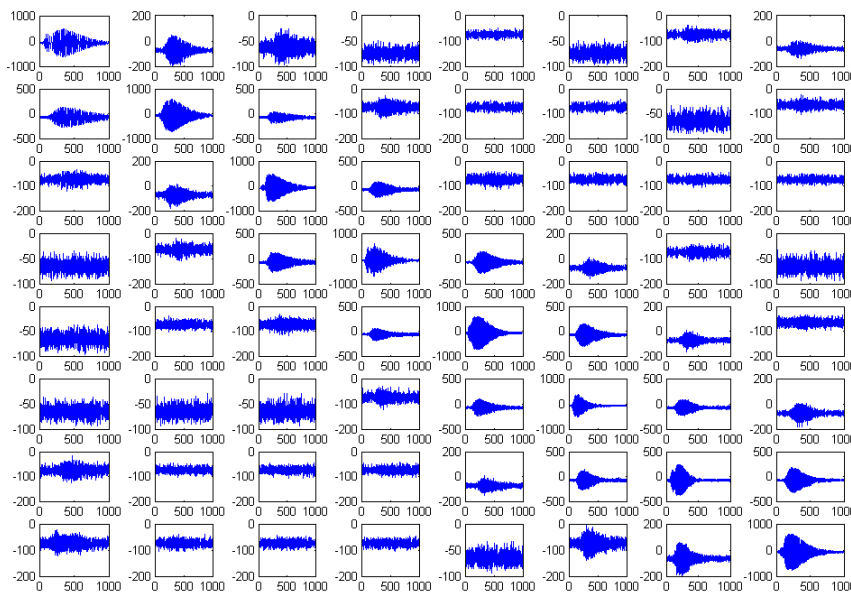


Figure 7.6: Test Subject: Wooden Pole - raw sampled signals

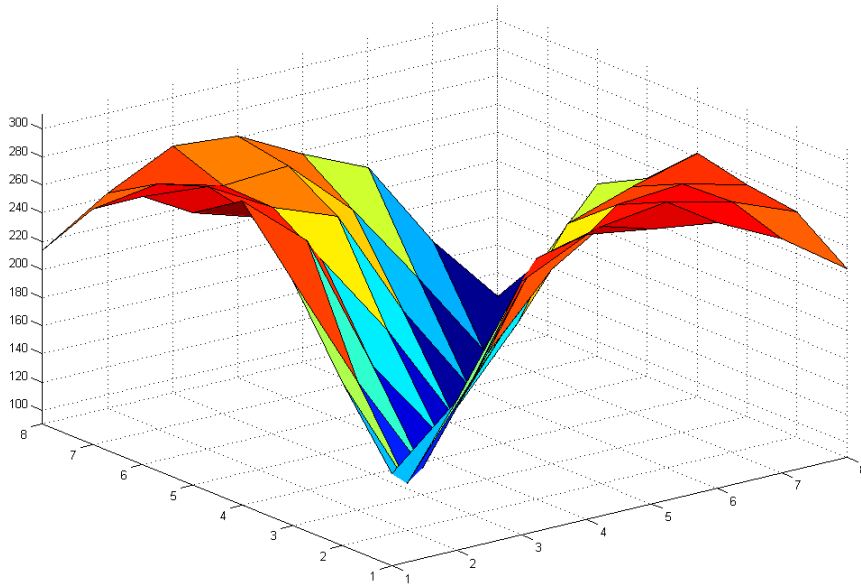


Figure 7.7: Test Subject: Empty space - surface plot of TOF values

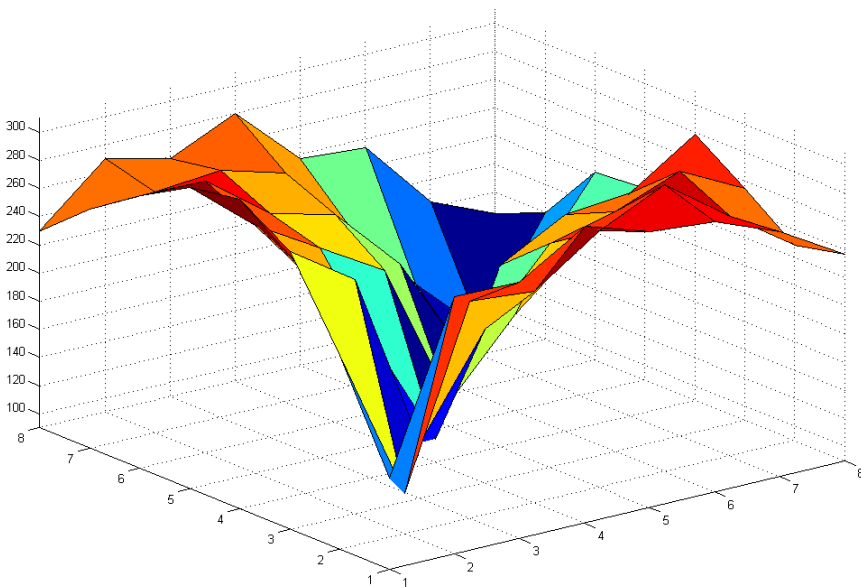


Figure 7.8: Test Subject: Red Bottle - surface plot of TOF values

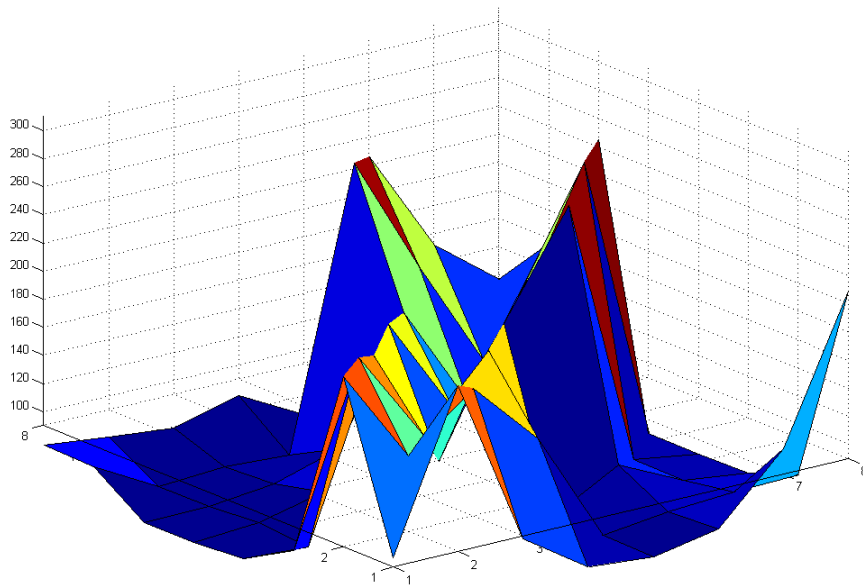


Figure 7.9: Test Subject: Wooden Pole - surface plot of TOF values

Chapter 8

Conclusions

After considering the results acquired from testing the system, it is evident that the overall data acquisition unit works precisely as planned according to the specifications in chapter 4. The high resolution 12 bit signal sampling as well as the relatively high speed at which the peripheral board operates, demonstrate that the system is capable of extracting high quality information from the testing environment.

It is clear that the digital side of the system works extremely well, and has vast room for increased speed and exploitation of its resolution. The processing in Matlab produced valid results that correlated well to expected readings. However the results obtained also demonstrated that the signals arriving at the ADC are not calibrated to exploit the full-scale input range of the device. The reasons for this include a weak transmission signal with a maximum peak-to-peak output of 7.5V at the transmitters. This signal is attenuated to such an extent through dense material such as wood that only noise is read at the receiver end. Another reason is lack of gain at the receiver end. The design choice of using the PGA to reduce circuit size meant a weak maximum gain of 32 which proved inadequate for preparing received analogue signals to be fed into the ADC.

Another point of note is the speed at which the whole scanning process occurs . The entire 64 sets of 1000 samples took less than 1 second to collect each time a target was scanned. However the process of getting this data back to the PC to be processed is slow and very manual, as are the Matlab DSP procedures. The end visualization depends only on the TOF values. Thus it can easily be seen how the only data that should be sent back from the FPGA to the PC or laptop, should be the TOF values, meaning the digital signal processing should take place entirely on-board the FPGA. This could potentially provide the capabilities for a real-time ultrasound tomography device. This was however foreseen, and the final conclusion is that the implemented system provides an excellent framework for future work into a soft-core DSP block.

Chapter 9

Recommendations and Proposals

Considering the conclusions discussed in chapter 8, the following extensions to this topic are proposed:

- An overhaul of the analogue side of the system implemented in this project. The goals of which would be to:
 - generate much more powerful ultrasound waves at the source transducers
 - provide more gain at the receiving end.
 - provide for more transducers in the array (at least 16), giving more propagation paths and greater resolution.
 - redesign the transducer housing for greater stability and directional accuracy
- To design and implement a soft-core digital signal component that can be programmed into the FPGA alongside the Nios II processor to facilitate real-time digital signal processing. This should specifically include (see figure 9.1 for an illustration):
 - a signal generation core that should generate a predefined digital signal and feed this out to the DAC at a constant specified sample rate.
 - a DSP core that would interface directly to the external ADC and would read in samples and clock the ADC at a constant specified sampling rate. The unit should process the received signal in real-time, and extract the TOF values which could then be passed to the Nios II processor.
 - the compatibility of the above two components with the Nios II Avalon Bus.
- To integrate ethernet capabilities into the system. This would allow the FPGA device and peripheral board to operate in a location that is remote from the place where the extracted data is visualized. This could be done quite easily with the Nios II , a proper FPGA Development kit (instead of the Evaluation Kit) and appropriate licenses.

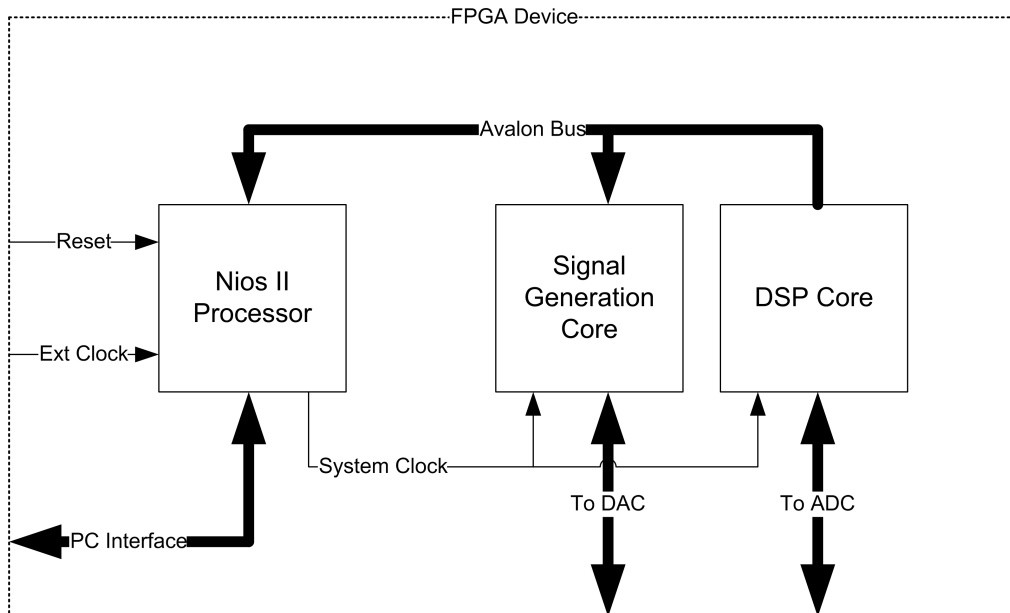
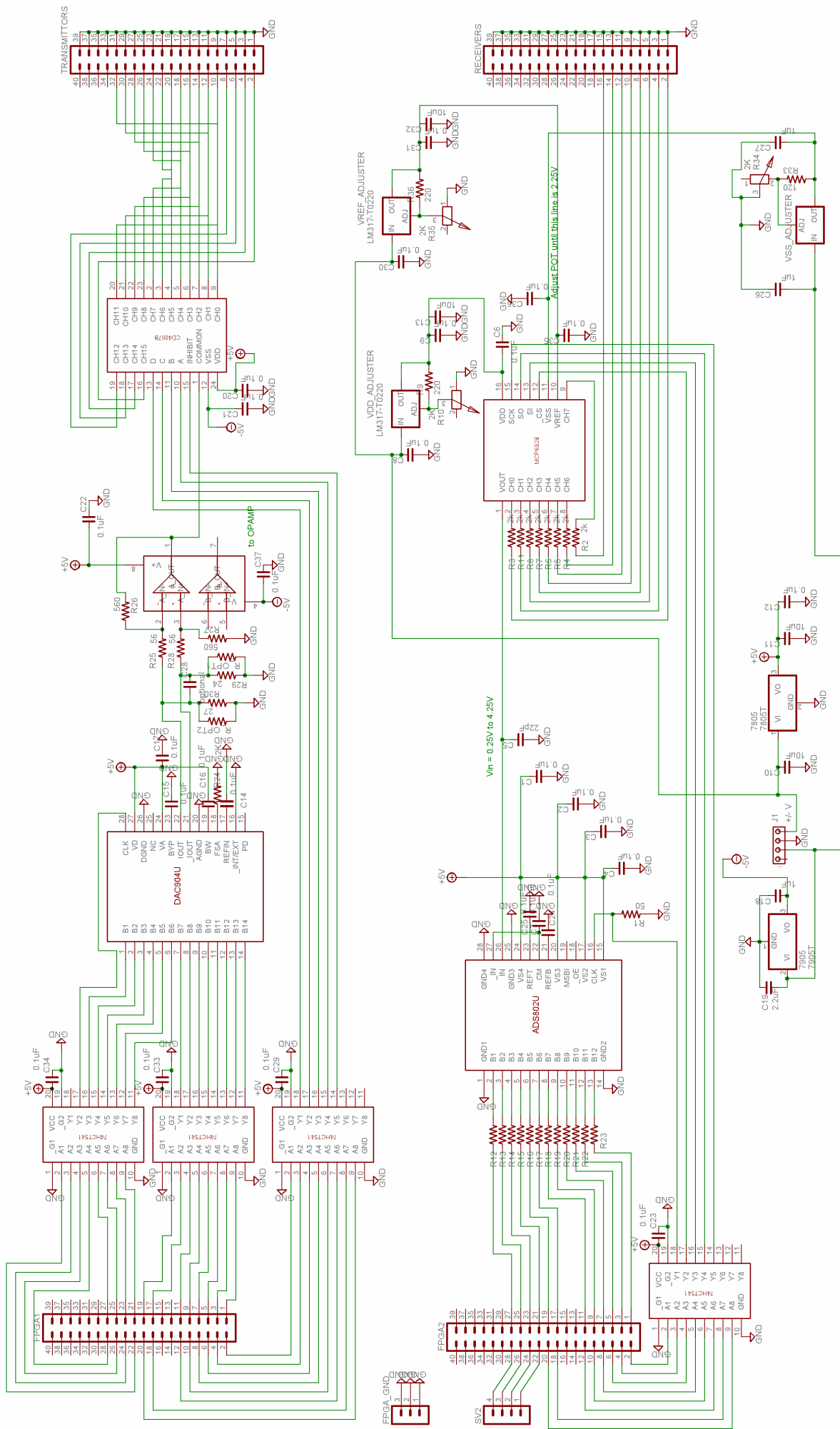


Figure 9.1: Proposed signal generation and DSP core configuration

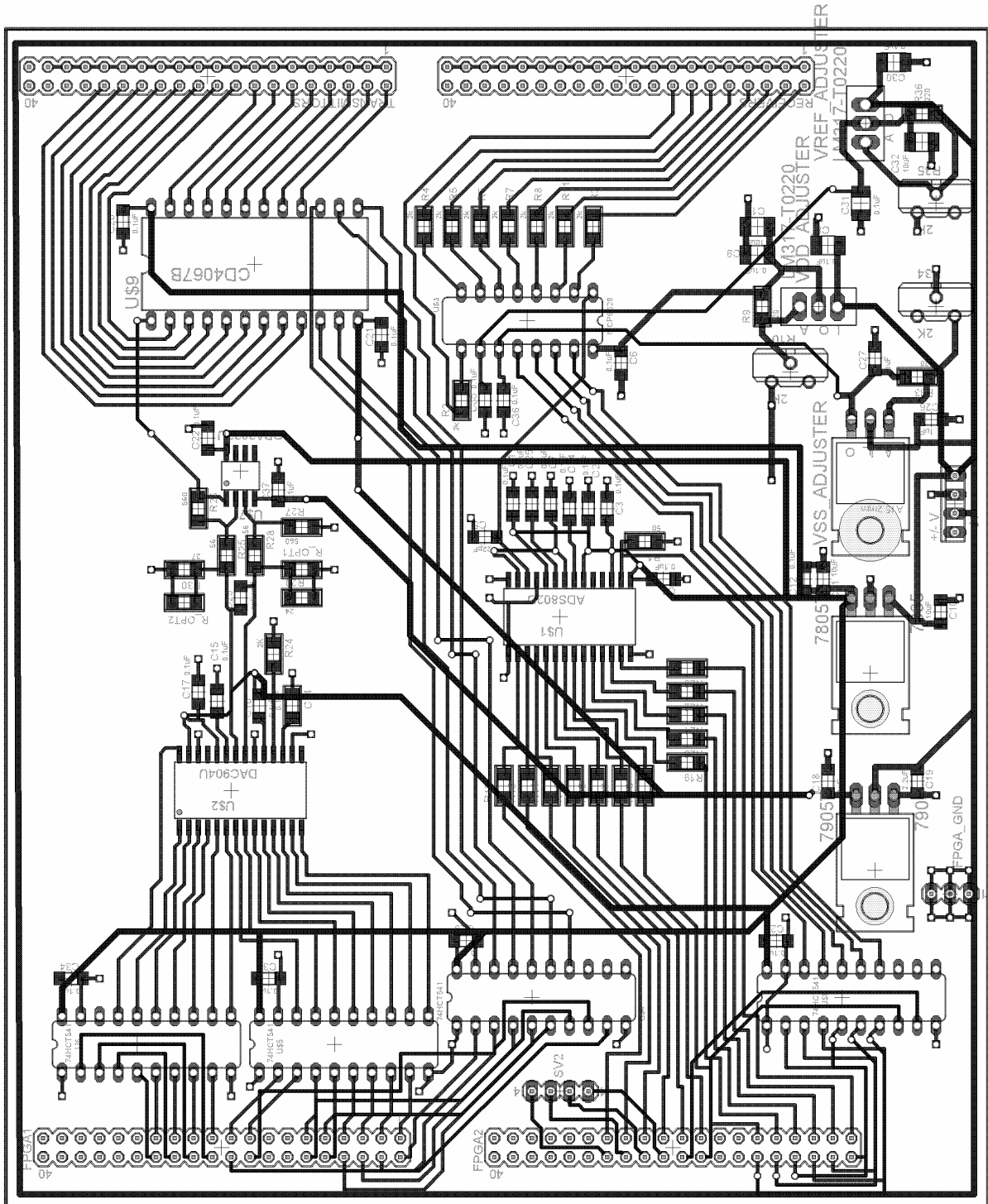
Appendix A

Peripheral Board Schematic



Appendix B

Peripheral Board Assembly



Appendix C

Software Source Code

The following is the C code that was written in the Nios II IDE and executed on the Nios II processor. Note the library generated HAL and associated libraries are not included.

```
/****** control.c *****/
#include <stdio.h>
#include <math.h>
#include <string.h>
#include <unistd.h>
#include "system.h"
#include "sys/alt_irq.h"
#include "altera_avalon_pio_regs.h"
#include "altera_avalon_spi.h"
#include "sys/alt_timestamp.h"
#include "alt_types.h"
#define PI 3.141592653 //Value of Pi
#define DAC_SAMPLES 100 //Number of DAC Samples to generate
#define ADC_SAMPLES 1000 //Number of ADC Samples to capture
#define DAC_RESOLUTION 16384 //2^14 bits is 16384 in decimal
#define FREQ 40500 //The desired frequency of the generated ultrasound wave
#define MAX_FREQ 1266666 //This is the maximum output switching
//freq the hardware is capable of.

#define NUM_INPUT_CHANNELS 8
#define NUM_OUTPUT_CHANNELS 8
static alt_u16 ADC_Data[NUM_INPUT_CHANNELS][NUM_OUTPUT_CHANNELS][ADC_SAMPLES];
static alt_u16 DAC_Data[DAC_SAMPLES];
static void clock_ADC() //clocks the ADC by one cycle.
{
    IOWR_ALTERA_AVALON_PIO_DATA(ADC_CLK_BASE,0xf);
    IOWR_ALTERA_AVALON_PIO_DATA(ADC_CLK_BASE,0x0);
}
static void clock_DAC() //clocks the DAC by one cycle.
{
    IOWR_ALTERA_AVALON_PIO_DATA(DAC_CLK_BASE,0xf);
    IOWR_ALTERA_AVALON_PIO_DATA(DAC_CLK_BASE,0x0);
}
static void set_gain(int gain)
{
    alt_u8 wdata[2];
    alt_u8 rdata[4];
    wdata[0] = 0x40;
    switch (gain)
    {
        case 1:
            wdata[1] = 0x00;
```

```

        break;
    case 2:
        wdata[1] = 0x01;
        break;
    case 4:
        wdata[1] = 0x02;
        break;
    case 5:
        wdata[1] = 0x03;
        break;
    case 8:
        wdata[1] = 0x04;
        break;
    case 10:
        wdata[1] = 0x05;
        break;
    case 16:
        wdata[1] = 0x06;
        break;
    case 32:
        wdata[1] = 0x07;
        break;
    default:
        wdata[0] = 0x00;
}
alt_avalon_spi_command(SPI_BASE, 0, 2, wdata, 0, rdata, 0);
}
static void set_input_channel(unsigned int chan)
{
    alt_u8 wdata[2];
    alt_u8 rdata[4];
    wdata[0] = 0x41;
    switch (chan)
    {
        case 0:
            wdata[1] = 0x00;
            break;
        case 1:
            wdata[1] = 0x01;
            break;
        case 2:
            wdata[1] = 0x02;
            break;
        case 3:
            wdata[1] = 0x03;
            break;
        case 4:
            wdata[1] = 0x04;
            break;
        case 5:
            wdata[1] = 0x05;
            break;
        case 6:
            wdata[1] = 0x06;
            break;
        case 7:
            wdata[1] = 0x07;
            break;
        default:
            wdata[0] = 0x00;
    }
    alt_avalon_spi_command(SPI_BASE, 0, 2, wdata, 0, rdata, 0);
}

```

```

}
static void set_output_channel(unsigned int chan)
{
    alt_u8 temp = chan & 0xf;
    IOWR_ALTERA_AVALON_PIO_DATA(DEMUX_SELECT_BASE,temp);
}
static void generate_sine_wave(int freq) //fills the DAC array with a sine wave
{
    int count;
    double temp;
    double samples_per_oscillation = ((double)MAX_FREQ / (double)freq);
    double delta_t = (1 / (double)(MAX_FREQ));
    unsigned int multiplier = DAC_RESOLUTION / 2;
    printf("Sine Wave: samples_per_oscillation = %f \n",samples_per_oscillation);
    printf("Sine Wave: delta_t = %f seconds \n",delta_t);
    printf("Sine Wave: multiplier = %u seconds \n",multiplier);
    printf("Sine Wave: Generating %f seconds of sound\n", (delta_t * DAC_SAMPLES));
    for (count = 0; count < DAC_SAMPLES; count++)
    {
        temp = sin(2*PI*freq*delta_t*count);
        temp = temp * multiplier;
        temp = temp + multiplier;
        DAC_Data[count] = (unsigned int)floor(temp);
    }
    printf("Sample of generated data:\n");
    for (count = 0; count < 20;count ++)
    {
        printf("data[%d] = %u\n",count, (unsigned int)DAC_Data[count]);
    }
}
static void stabilize()
{
    IOWR_ALTERA_AVALON_PIO_DATA(DAC_OUT_BASE,0x2000);
    clock_DAC();
    clock_ADC();
    clock_ADC();
    clock_ADC();
    clock_ADC();
    clock_ADC();
    clock_ADC();
    clock_ADC();
}
static void perform_scan()
{
    register unsigned int count;
    unsigned int outer,inner;

    //Steady both DAC and ADCs for transmission
    stabilize();
    usleep(1000);

    for (outer = 0; outer < NUM_OUTPUT_CHANNELS; outer++)
    {
        set_output_channel(outer);
        for (inner = 0; inner < NUM_INPUT_CHANNELS; inner++)
        {
            set_input_channel(inner);
            usleep(10000); //wait for voltages to settle
            for (count = 0; count < DAC_SAMPLES; count++)
            {
                IOWR_ALTERA_AVALON_PIO_DATA(DAC_OUT_BASE,DAC_Data[count]);
                clock_DAC();
            }
        }
    }
}

```

```

        for (count = 0; count < ADC_SAMPLES; count++)
        {
            clock_ADC();
            ADC_Data[inner][outer][count] = IORD_ALTERA_AVALON_PIO_DATA(ADC_IN_BASE);
        }
        printf("Acquired: OutChan[%d],InChan[%d]\n",outer,inner);
        stabilize();
        usleep(1000);
    }
}
}
void print_results_binary()
{
    unsigned int outer,inner;
    FILE* fp = NULL;

    printf("Attempting to Open data_bin ..... \n");
    fp = fopen ("/mnt/host/data.bin", "w");
    if (fp == NULL)
    {
        printf ("Cannot open file data.bin\n");
    }
    else
    {
        printf("Writing array values....\n");
        for (outer = 0; outer < NUM_INPUT_CHANNELS;outer++)
        {
            for (inner = 0; inner < NUM_OUTPUT_CHANNELS; inner++)
            {
                fwrite(ADC_Data[outer][inner],2,ADC_SAMPLES,fp);
            }
        }
        printf("Closing file.....\n");
        fclose (fp);
        printf("File Closed and Saved. \n");
    }
}
int main(void)
{
    FILE* fp;
    char str[20] = "";
    int count;

    //Steady both DAC and ADCs for transmission
    clock_ADC();
    IOWR_ALTERA_AVALON_PIO_DATA(DAC_OUT_BASE,0x2000);
    clock_DAC();

    printf("Generating Sine table....\n");
    generate_sine_wave(FREQ);
    printf(".....Done\n");

    /* Perform any necessary initialization commands */
    clock_DAC();
    clock_ADC();

    fp = fopen ("/dev/jtag_uart", "r+"); //Open jtag-out for reading and writing
    while (1)
    {
        printf("Please enter a command:\n");
        fgets(str,10,fp);
    }
}

```

```

if (!strcmp("g2\n", str))
{
    printf("Changed Gain to: 2\n");
    set_gain(2);
}
else if (!strcmp("g1\n", str))
{
    printf("Changed Gain to: 1\n");
    set_gain(1);
}
else if (!strcmp("g4\n", str))
{
    printf("Changed Gain to: 4\n");
    set_gain(4);
}
else if (!strcmp("g5\n", str))
{
    printf("Changed Gain to: 5\n");
    set_gain(5);
}
else if (!strcmp("g8\n", str))
{
    printf("Changed Gain to: 8\n");
    set_gain(8);
}
else if (!strcmp("g10\n", str))
{
    printf("Changed Gain to: 10\n");
    set_gain(10);
}
else if (!strcmp("g16\n", str))
{
    printf("Changed Gain to: 16\n");
    set_gain(16);
}
else if (!strcmp("g32\n", str))
{
    printf("Changed Gain to: 32\n");
    set_gain(32);
}
else if (!strcmp("scan\n", str))
{
    printf("Peforming Scan.....\n");
    perform_scan();
    printf(".....Done\n");
}
else if (!strcmp("print\n", str))
{
    print_results_binary();
}
}
return(0);
}

```


Appendix D

Matlab Functions

D.1 readBin.m

```
function [data] = readBin(filename)
ADC_samples = 1000;
out_channels = 8;
in_channels = 8;
fid = fopen(filename,'rb');
A = fread(fid, inf, 'uint16');
fclose(fid);
figure
for I = 1:1:in_channels
    for J = 1:1:out_channels
        for count = 1:1:ADC_samples
            data(I,J,count) = A((I*8-8+J)*1000-1000 + count) - 2048;
            temp(count) = A((I*8-8+J)*1000-1000 + count) - 2048;
        end
        subplot(8,8,I*8-8+J);
        plot(temp)
    end
end
end
```

D.2 extractSampling.m

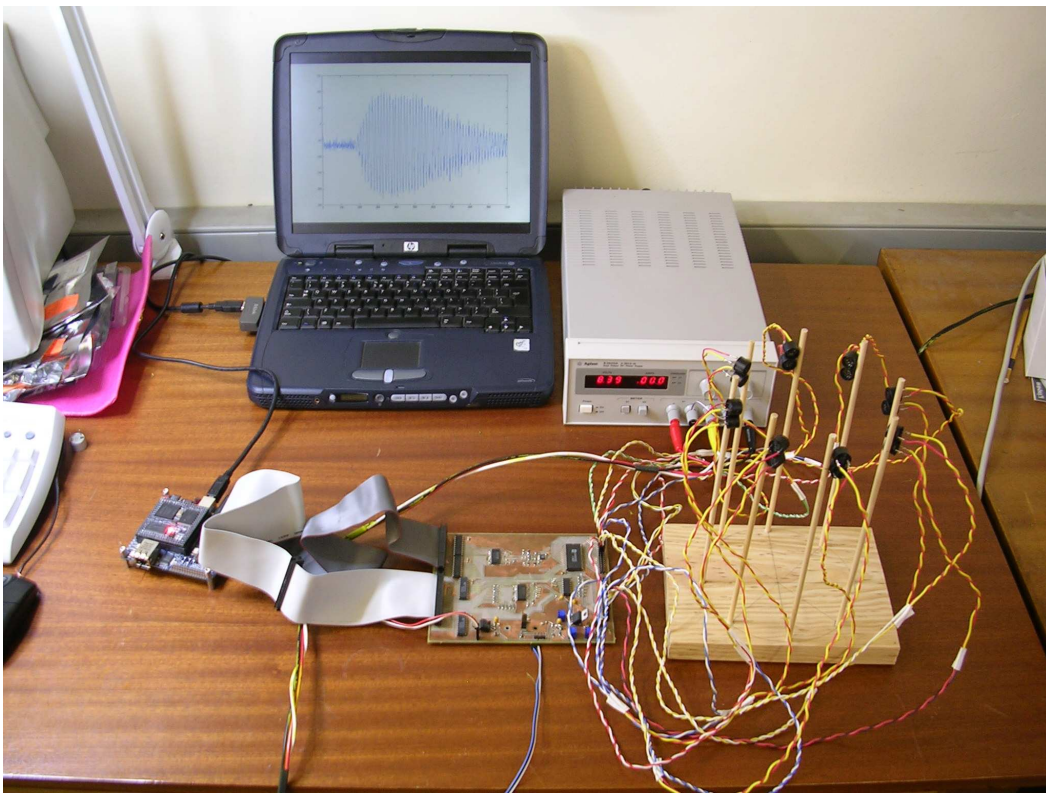
```
function [data] = extractSampling(array,in_chan,out_chan)
ADC_samples = 1000;
for I = 1:1:ADC_samples
    data(I) = array(in_chan,out_chan,I);
end
```

D.3 findTOF.m

```
function [TOF] = findTOF(data)
ADC_samples = 1000;
in_channels = 8;
out_channels = 8;
figure
for i=1:1:in_channels
    for j = 1:1:out_channels
        temp = extractSampling(data,i,j);
        spec = fft(temp);
        spec(1) = 0;
        for count=(ADC_samples/2 + 1):1:ADC_samples
            spec(count) = 0;
        end
        temp = abs(ifft(spec));
        temp = smooth(temp);
        subplot(8,8,i*8-8+j);
            plot(temp)
        x = ADC_samples;
        threshold = max(temp) / 2;
        for count = 50:1:ADC_samples
            if (temp(count) > threshold)
                x = count;
                break;
            end
        end
        TOF(i,j) = x;
    end
end
end
```

Appendix E

Photograph of the final system



Bibliography

- [1] *Field Programmable Gate Array*, Wikipedia, <http://en.wikipedia.org/wiki/FPGA>, October 2006
- [2] Discussions with Dr AJ Wilkinson (thesis supervisor)- Department of Electrical Engineering, University of Cape Town, 2006
- [3] David Pellerin, Scott Thibault, *Practical FPGA Programming in C*, Chapter 1, Prentice Hall 2005
- [4] M. Morris Mano, Charles R. Kime, *Logic and Computer Design Fundamentals 2nd Edition Updated*, Chapter 6, Prentice Hall 2001
- [5] *System-on-a-Chip*, Wikipedia, <http://en.wikipedia.org/wiki/System-on-a-chip>, October 2006
- [6] *Digital Set-Top Boxes & Integrated Digital Television Systems*, Altera Corporation, <http://www.altera.com/end-markets/consumer/dtv/csm-digitaltv.html>, October 2006
- [7] *Ultrasound Tomography*, Zunaïd Parker, University of Cape Town, October 2005
- [8] *Ultrasound*, Wikipedia, <http://en.wikipedia.org/wiki/Ultrasound>, October 2006
- [9] *Sound*, Wikipedia, <http://en.wikipedia.org/wiki/Sound>, October 2006
- [10] *Datasheet - DAC904*, <http://www.ti.com>, August 2006
- [11] *Datasheet - MCP6S28*, <http://www.microchip.com>, August 2006
- [12] *Datasheet - ADS802*, <http://www.ti.com>, August 2006
- [13] *Nios II Evaluation Kit - Bundled Documentation*, <http://www.altera.com>, August 2006
- [14] *Nios II*, Wikipedia, http://en.wikipedia.org/wiki/Nios_II, September 2006
- [15] *Nios II Software Developer's Handbook*, <http://www.altera.com>, August 2006
- [16] *Nios II Processor Reference Handbook*, <http://www.altera.com>, August 2006